



Swansea University  
Prifysgol Abertawe



## Cronfa - Swansea University Open Access Repository

---

This is an author produced version of a paper published in :  
*Composite Structures*

Cronfa URL for this paper:  
<http://cronfa.swan.ac.uk/Record/cronfa30718>

---

### **Paper:**

Adhikari, S. (in press). Stochastic natural frequency analysis of damaged thin-walled laminated composite beams with uncertainty in micromechanical properties. *Composite Structures*  
<http://dx.doi.org/10.1016/j.compstruct.2016.10.035>

---

This article is brought to you by Swansea University. Any person downloading material is agreeing to abide by the terms of the repository licence. Authors are personally responsible for adhering to publisher restrictions or conditions. When uploading content they are required to comply with their publisher agreement and the SHERPA RoMEO database to judge whether or not it is copyright safe to add this version of the paper to this repository.  
<http://www.swansea.ac.uk/iss/researchsupport/cronfa-support/>

## Accepted Manuscript

Stochastic natural frequency analysis of damaged thin-walled laminated composite beams with uncertainty in micromechanical properties

S. Naskar, T. Mukhopadhyay, S. Sriramula, S. Adhikari

PII: S0263-8223(16)31051-0

DOI: <http://dx.doi.org/10.1016/j.compstruct.2016.10.035>

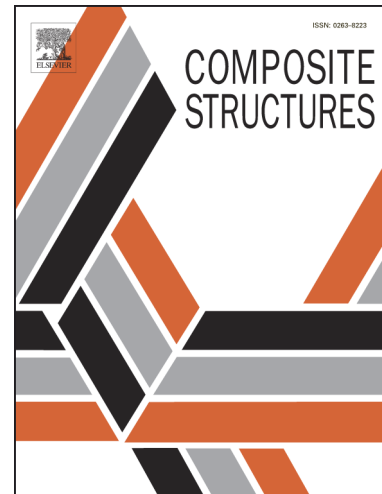
Reference: COST 7861

To appear in: *Composite Structures*

Received Date: 27 June 2016

Revised Date: 14 October 2016

Accepted Date: 15 October 2016



Please cite this article as: Naskar, S., Mukhopadhyay, T., Sriramula, S., Adhikari, S., Stochastic natural frequency analysis of damaged thin-walled laminated composite beams with uncertainty in micromechanical properties, *Composite Structures* (2016), doi: <http://dx.doi.org/10.1016/j.compstruct.2016.10.035>

This is a PDF file of an unedited manuscript that has been accepted for publication. As a service to our customers we are providing this early version of the manuscript. The manuscript will undergo copyediting, typesetting, and review of the resulting proof before it is published in its final form. Please note that during the production process errors may be discovered which could affect the content, and all legal disclaimers that apply to the journal pertain.

## Stochastic natural frequency analysis of damaged thin-walled laminated composite beams with uncertainty in micromechanical properties

S. Naskar<sup>a\*</sup>, T. Mukhopadhyay<sup>b</sup>, S. Sriramula<sup>a</sup>, S. Adhikari<sup>b</sup>

<sup>a</sup>*LRF Centre for Safety & Reliability Engineering, School of Engineering, University of Aberdeen, Aberdeen, UK*

<sup>b</sup>*College of Engineering, Swansea University, Swansea, UK*

### Abstract

This paper presents a stochastic approach to study the natural frequencies of thin-walled laminated composite beams with spatially varying matrix cracking damage in a multi-scale framework. A novel concept of stochastic representative volume element (SRVE) is introduced for this purpose. An efficient radial basis function (RBF) based uncertainty quantification algorithm is developed to quantify the probabilistic variability in free vibration responses of the structure due to spatially random stochasticity in the micro-mechanical and geometric properties. The convergence of the proposed algorithm for stochastic natural frequency analysis of damaged thin-walled composite beam is verified and validated with original finite element method (FEM) along with traditional Monte Carlo simulation (MCS). Sensitivity analysis is carried out to ascertain the relative influence of different stochastic input parameters on the natural frequencies. Subsequently the influence of noise is investigated on radial basis function based uncertainty quantification algorithm to account for the inevitable variability for practical field applications. The study reveals that stochasticity/ system irregularity in structural and material attributes affects the system performance significantly. To ensure robustness, safety and sustainability of the structure, it is very crucial to consider such forms of uncertainties during the analysis.

**Keywords:** damaged composite laminates; stochastic representative volume element (SRVE); uncertainty quantification; radial basis function; stochastic natural frequency; sensitivity analysis

---

\* Corresponding author: Susmita Naskar

E-mail: r01sn15@abdn.ac.uk (S. Naskar); 800712@swansea.ac.uk (T. Mukhopadhyay)

URL: www.susmitanaskar.com (S. Naskar); www.tmukhopadhyay.com (T. Mukhopadhyay)

## 1. Introduction

Laminated composites have gained huge popularity because of their weight sensitivity, high-strength and stiffness to weight ratios and long-term cost effectiveness. Such structures are extensively used in aerospace, marine, construction and other industries due to their application specific tailorable material properties. It is widely known that thin walled composite beams are used broadly in various applications of structural engineering, such as helicopter blades, wings, trusses in space structures, submarine hulls, cooling tower shafts, medical tubing, connecting shafts, transmission poles, tail boom of helicopter and tube like structures in missiles. Because of their inherent complexity, a laminated composite beam is difficult to manufacture accurately according to its exact design specifications, resulting in undesirable uncertain responses due to random material and geometric properties. Generally uncertainties are broadly classified into three divisions, namely aleatoric (because of variability in the structural system parameters), epistemic (because of lack of information of the structural system) and prejudicial (because of the absence of variability characterization) [1-3]. The performances of composite structures are influenced by the quality control processes, operating conditions and environmental effects. It can be observed that there are uncertainties in input forces, system descriptions, computation as well as model calibration. The production of composite laminates is subjected to large variability because of unavoidable fabricating imperfections, operational factors, inaccurate experimental data, lack of experience etc. Furthermore, because of various forms of damages and defects, effective material properties may vary substantially from the specified values. As a cumulative effect, the vibration characteristics of such composite structures show significant variability from the deterministic values. Therefore, the structural performance is subjected to a significant element of risk from safety and serviceability point of view. Moreover, uncertainties in input parameters can propagate through different modelling scales and influence other parameters and the final system output can have a substantial cascading effect because of the accumulation of the risk [4]. Such variability can result in significant deviations from the

expected outputs (deterministic design values). Hence, it is of prime importance to characterize the probability distribution of the response parameters of interest (such as natural frequencies) by accounting for the variability in stochastic input parameters.

Since late eighties, research activities are dedicated towards the development of appropriate analysis for thin-walled composite beams [5-6]. Bauld and Tseng [7] studied the static structural behavior of a thin-walled composite orthotropic member under various load patterns. Bauchau [8] studied thin walled composite beam models with effects of shear deformability. Cortínez and Piovan reported vibration and buckling analysis of thin-walled composite beams with shear deformability [9]. Various other studies on composite beams are found to be concentrated on deterministic analysis concerning statics and dynamic responses including aero-elastic effects [10-16]. An extensive review of literature on laminated composites reveals that most of the studies carried out so far are based on a deterministic framework, in spite of the possibility of significant probabilistic variability in the responses of such structures due to inevitable stochasticity in material and geometric parameters. Recently attempts have been made to carry out stochastic analysis for different responses of composite plates and shells [17-19]. The treatment of uncertainties to quantify the same for thin walled circular composite beam has received little attention. Of late, Piovan *et al.* have investigated the effects of parametric uncertainty on dynamics of thin-walled laminated composite beams [20]. However, most of the recent research follows a random variable based approach that neglects the spatially random variation of material properties. Consideration of random fields for modelling uncertainty in composite structures is practically more relevant. Moreover, consideration of spatially varying damage that often develops in the operational environments has not been accounted in scientific literature yet.

This paper presents a realistic analysis on stochastic natural frequency of thin-walled laminated composite beams with spatially varying matrix cracking damage in a multi-scale framework. A typical schematic description of damage development in composite laminates is

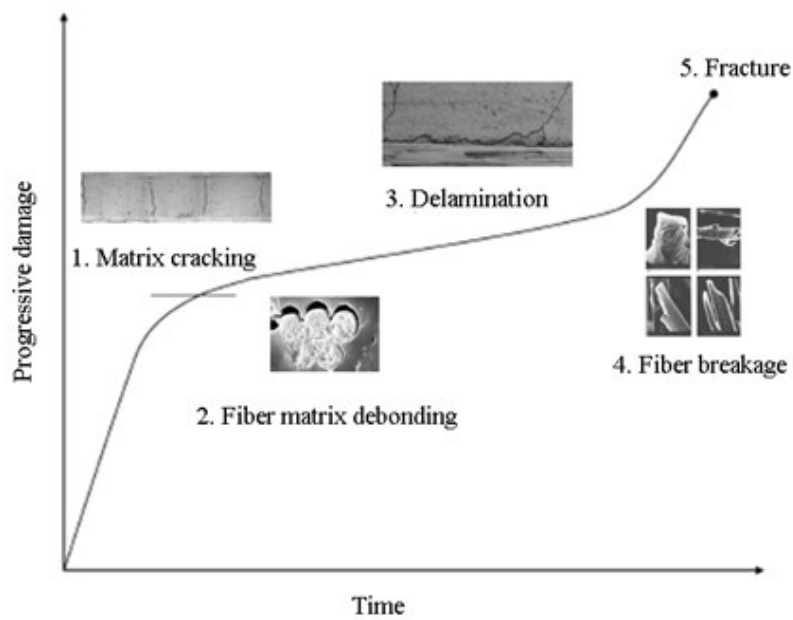


**Fig. 1** Occurrence of progressive damage in composites

depicted in Figure 1, where the five identifiable damage mechanisms are indicated in the order of their occurrence [21]. In the early stages of damage accumulation, multiple matrix cracking dominates in the layers which have fibres aligned transverse to the applied load direction. Static tensile tests on cross-ply laminates have shown that the transverse matrix cracks can initiate as early as at about 0.4-0.5% applied strain depending upon the laminate configuration. Thus in the present investigation, spatially random distribution of matrix cracking is considered along with other stochastic input parameters to characterize the natural frequencies of thin-walled composite beams. The crucial issue of expensive computation involved in uncertainty quantification of composite structures and the development of radial basis function based uncertainty quantification algorithm to mitigate this lacuna is discussed in the following paragraph.

One of the most prominent approaches followed for uncertainty quantification in composite structures is the Monte Carlo simulation (MCS) based approach. MCS is a computerized mathematical technique which allows to account for risk in quantitative analysis and decision making. This technique is mainly utilized to generate the uncertain variable output

frequency using large number of samples. MCS technique can be broadly used to quantify the uncertainty of laminated composites in which thousands of FEM simulations are required to be carried out. Therefore, this technique has limited practical use because of its computational intensiveness unless some form of efficient modelling technique is applied to mitigate this lacuna. Moreover, due to consideration of matrix cracking damage in the present analysis, the entire process of obtaining natural frequency for a particular realization of Monte Carlo sample becomes a multi-step procedure (in the first step of the analysis, the effective material properties of damaged composite are obtained; subsequently these effective material properties are fed in the finite element model to compute global mass and stiffness matrices and thereby the natural frequencies) making it even more time consuming. An efficient radial basis function [22-23] based uncertainty quantification approach is developed in this article to quantify the probabilistic variability in free vibration responses of the structure due to spatially random stochasticity in the micro-mechanical and geometric properties along with matrix-cracking damage. In the present approach, the effect of uncertainty is accounted in the elementary micro-level first and then these effects are disseminated towards the global responses via surrogates of the actual FEM models.

To the best of the authors' knowledge, there is no scientific literature available which deals with stochastic structural dynamics based on radial basis function for uncertainty quantification of thin-walled composite beams including the effect of matrix cracking in a probabilistic approach. Moreover, consideration of spatially random variability of the stochastic input parameters for laminated composites is very scarce to find in available literature. The present paper concentrates on these identified lacunas concerning the free vibration analysis of thin-walled composite beams. A novel concept of stochastic representative volume element (SRVE) is introduced in this article. Besides random-field based stochastic analysis of natural frequencies following a multi-scale framework, this article presents the effect of inevitable noise in RBF based uncertainty quantification algorithm to simulate the uncertainties associated

with the actual field condition. This paper hereafter is organized as follows, Section 2: governing equations of thin walled composite beams including the effect of matrix cracking; Section 3: brief description of RBF based surrogate modelling; Section 4: RBF based approach coupled with the concept of SRVE for probabilistic characterization of natural frequencies and the algorithm to quantify the effect of noise; Section 5: results and discussion; Section 6: summary of results and perspective of the present work in the context to other contemporary researches in relevant fields and Section 7: conclusion.

## 2. Governing Equations for thin walled composite beam with matrix cracking damage

Nuismer and Tan's [24] work on matrix cracking in composites is extended to a spatially random stochastic framework for studying the free vibration response of a thin-walled composite beam following a novel SRVE approach. To obtain the expression for equivalent elastic properties, a composite thin walled beam under general in-plane stochastic loading  $[\overline{\sigma}_x, \overline{\sigma}_y, \overline{\tau}_{xy}](\overline{\omega})$  is considered, where  $\overline{\omega}$  represents the stochastic character. The matrix cracks are assumed to exist in the central lamina group as shown in the Figure 2(a). The analysis has been carried out by considering uniform crack spacing of  $2L$  in the central composite lamina. A symmetry along the mid-plane of the laminate is considered, due to which only one quarter can be analysed. The modelled portion (as shown in Figure 2(b)) of the length  $L$  has been divided into two sublaminates, wherein sublaminate 1 denotes the central lamina ply group and sublaminate 2 denotes the outer lamina ply group. The assumed uniformity of the load, geometry and material properties have been considered along the  $y$  axis where the displacements can be obtained from the following equations [24],

$$u^i(\overline{\omega}) = u^i(x, z)(\overline{\omega}) \quad (1)$$

$$v^i(\overline{\omega}) = y(\overline{\omega})\varepsilon_y(\overline{\omega}) + v^i(x, z)(\overline{\omega}) \quad (2)$$

$$w^j(\overline{\omega}) = w^j(x, z)(\overline{\omega}) \quad (3)$$

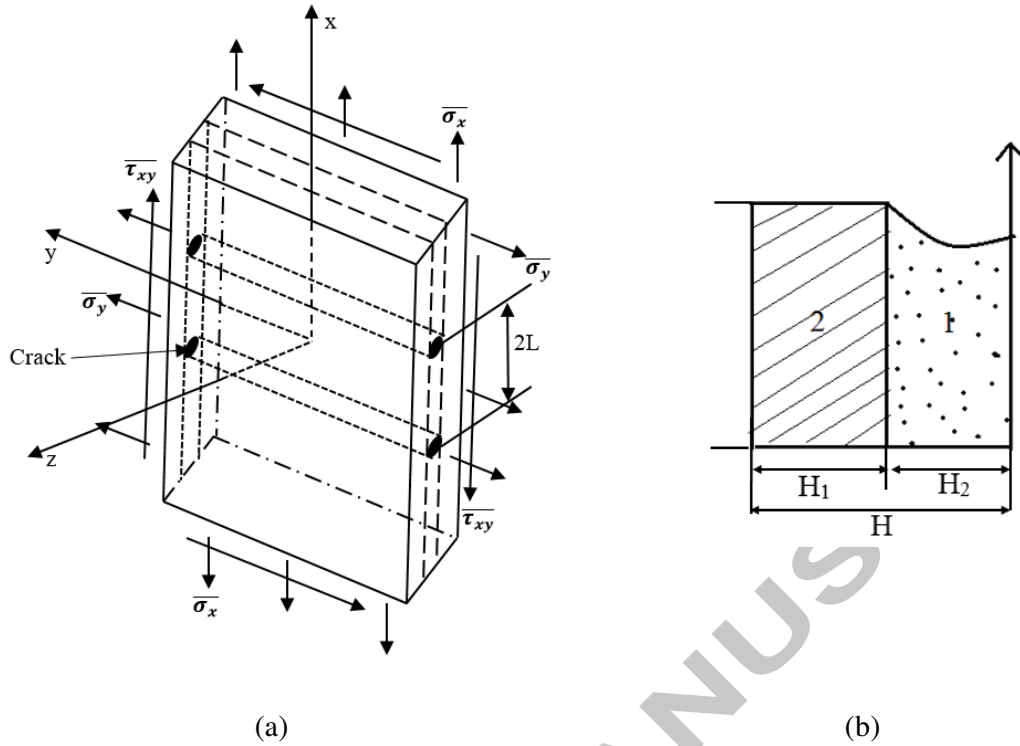


**Fig. 2** (a) Laminated composite containing cracked ply; (b) One-quarter of laminated composite unit-cell

where,  $\varepsilon_y$  denotes the uniform strain along  $y$ -direction and subscript  $i$  denotes the material ply 1 and 2. The homogenized properties across the lamina thickness can be expressed as,

$$(\bar{X}(\bar{\omega}))^i = \frac{1}{H_i(\bar{\omega})} \int_{H_i(\bar{\omega})} (X(\bar{\omega}))^i dz \quad (4)$$

where a bar is used to indicate the through-the-thickness average of the variable  $X$  and the subscript  $i$  which refers to sublaminates 1 or 2. A simple linear variation of the out of plane shear stress across the lamina thickness is assumed. In the present study,  $[\pm\theta_m/90_n]_s$  configuration of laminate is considered for the purpose of analysis. Nuismer and Tan [24] found that the solution of the in-plane normal response of composite laminate decouples from the solution of the in plane shear response due to the assumption of the orthotropy of the laminates and that is why each of the response i.e. normal and shear are considered separately. Therefore, the reduced laminate stiffness matrix which is having the effect of the matrix cracking in  $90^\circ$  ply group is given by the following equation [24],

$$\dot{A}(\bar{\omega}) = \begin{bmatrix} \dot{A}_{11}(\bar{\omega}) & \dot{A}_{12}(\bar{\omega}) & 0 \\ \dot{A}_{12}(\bar{\omega}) & \dot{A}_{22}(\bar{\omega}) & 0 \\ 0 & 0 & \dot{A}_{66}(\bar{\omega}) \end{bmatrix} \quad (5)$$

where the terms of the above matrix can be written as following,

$$\dot{A}_{11}(\bar{\omega}) = \frac{H_1(\bar{\omega})\dot{Q}_{11}^{(1)}(\bar{\omega}) + H_2(\bar{\omega})\dot{Q}_{11}^{(2)}(\bar{\omega})}{\beta_2(\bar{\omega})H(\bar{\omega})} \quad (6)$$

$$\dot{A}_{12}(\bar{\omega}) = \frac{\beta_1(\bar{\omega})H_1(\bar{\omega})\dot{Q}_{12}^{(1)}(\bar{\omega}) + \beta_2(\bar{\omega})H_2(\bar{\omega})\dot{Q}_{12}^{(2)}(\bar{\omega})}{\beta_2(\bar{\omega})H(\bar{\omega})} \quad (7)$$

$$\dot{A}_{22}(\bar{\omega}) = \frac{H_1(\bar{\omega})\dot{Q}_{22}^{(1)}(\bar{\omega}) + H_2(\bar{\omega})\dot{Q}_{22}^{(2)}(\bar{\omega})}{H(\bar{\omega})} - \left( \frac{\beta_2(\bar{\omega}) - \beta_1(\bar{\omega})}{\beta_2(\bar{\omega})} \right) \frac{H_1(\bar{\omega})}{H(\bar{\omega})} \frac{\dot{Q}_{12}^{(1)}(\bar{\omega})^2}{\dot{Q}_{11}^{(1)}(\bar{\omega})} \quad (8)$$

$$\dot{A}_{66}(\bar{\omega}) = \frac{H_1(\bar{\omega})\dot{Q}_{66}^{(1)}(\bar{\omega}) + H_2(\bar{\omega})\dot{Q}_{66}^{(2)}(\bar{\omega})}{\beta_4(\bar{\omega})H(\bar{\omega})} \quad (9)$$

where  $H$  is lamina thickness and  $Q_{ij}$  are the transformed layer stiffness components.

The values of  $\beta_1$ ,  $\beta_2$  and  $\beta_4$  are written below,

$$\beta_1(\bar{\omega}) = 1 - \frac{\tanh \alpha_1(\bar{\omega})L(\bar{\omega})}{\alpha_1(\bar{\omega})L(\bar{\omega})} \quad (10)$$

$$\beta_2(\bar{\omega}) = 1 + \frac{H_1(\bar{\omega})\dot{Q}_{11}^{(1)}(\bar{\omega})}{H_2(\bar{\omega})\dot{Q}_{11}^{(2)}(\bar{\omega})} \frac{\tanh \alpha_1(\bar{\omega})L(\bar{\omega})}{\alpha_1(\bar{\omega})L(\bar{\omega})} \quad (11)$$

$$\beta_4(\bar{\omega}) = 1 + \frac{H_1(\bar{\omega})\dot{Q}_{66}^{(1)}(\bar{\omega})}{H_2(\bar{\omega})\dot{Q}_{66}^{(2)}(\bar{\omega})} \frac{\tanh \alpha_2(\bar{\omega})L(\bar{\omega})}{\alpha_2(\bar{\omega})L(\bar{\omega})} \quad (12)$$

The values of  $\alpha_1$  and  $\alpha_2$  are given below,

$$\alpha_1^2(\bar{\omega}) = \frac{3\dot{Q}_{55}^{(1)}(\bar{\omega})\dot{Q}_{55}^{(2)}(\bar{\omega})}{H_1(\bar{\omega})\dot{Q}_{55}^{(1)}(\bar{\omega}) + H_1(\bar{\omega})\dot{Q}_{55}^{(2)}(\bar{\omega})} \left( \frac{H_1(\bar{\omega})\dot{Q}_{11}^{(1)}(\bar{\omega}) + H_2(\bar{\omega})\dot{Q}_{11}^{(1)}(\bar{\omega})}{H_1(\bar{\omega})H_2(\bar{\omega})\dot{Q}_{11}^{(1)}(\bar{\omega})\dot{Q}_{11}^{(2)}(\bar{\omega})} \right) \quad (13)$$

$$\alpha_2^2(\bar{\omega}) = \frac{3\dot{Q}_{44}^{(1)}(\bar{\omega})\dot{Q}_{44}^{(2)}(\bar{\omega})}{H_1(\bar{\omega})\dot{Q}_{44}^{(1)}(\bar{\omega}) + H_1(\bar{\omega})\dot{Q}_{44}^{(2)}(\bar{\omega})} \left( \frac{H_1(\bar{\omega})\dot{Q}_{66}^{(1)}(\bar{\omega}) + H_2(\bar{\omega})\dot{Q}_{66}^{(1)}(\bar{\omega})}{H_1(\bar{\omega})H_2(\bar{\omega})\dot{Q}_{66}^{(1)}(\bar{\omega})\dot{Q}_{66}^{(2)}(\bar{\omega})} \right) \quad (14)$$

The matrix  $\dot{A}(\bar{\omega})$  can be derived by averaging two of the sublaminates i.e.  $90^\circ$  ply group and  $\pm\theta^\circ$  ply group for accounting the effect of the matrix cracking which is the reduced matrix for the total laminate composite structure. Therefore the extensional stiffness matrix can be written as below,

$$A(\bar{\omega}) = t(\bar{\omega})\dot{A}(\bar{\omega}) \quad (15)$$

The coefficient of an orthotropic plate can be determined by using classical laminated theory [25-26]. The constitutive equation for the laminate is as follows:

$$\begin{Bmatrix} N(\bar{\omega}) \\ M(\bar{\omega}) \end{Bmatrix} = \begin{bmatrix} A(\bar{\omega}) & B(\bar{\omega}) \\ B(\bar{\omega}) & D(\bar{\omega}) \end{bmatrix} \begin{Bmatrix} \varepsilon(\bar{\omega}) \\ K(\bar{\omega}) \end{Bmatrix} \quad (16)$$

where,  $N$  and  $M$  denote the vectors of the three forces and three moments respectively, while  $\varepsilon$  and  $K$  are the vectors of strain and curvature and the stiffness coefficients  $A$ ,  $B$  and  $D$  correspond to membrane, coupling, and bending stiffness coefficient. The extensional stiffness matrix  $A$  can be obtained from Equation 15 and the extension bending stiffness matrix  $B$  is a null matrix for the case of symmetrical laminate structure. From the equideformability hypothesis [27], the following equation can be derived

$$\begin{Bmatrix} N_x(\bar{\omega}) \\ N_y(\bar{\omega}) \\ N_{xy}(\bar{\omega}) \end{Bmatrix} = \begin{bmatrix} A_{11}(\bar{\omega}) & A_{12}(\bar{\omega}) & A_{16}(\bar{\omega}) \\ A_{12}(\bar{\omega}) & A_{22}(\bar{\omega}) & A_{26}(\bar{\omega}) \\ A_{16}(\bar{\omega}) & A_{26}(\bar{\omega}) & A_{66}(\bar{\omega}) \end{bmatrix} \begin{Bmatrix} \varepsilon_x(\bar{\omega}) \\ \varepsilon_y(\bar{\omega}) \\ \varepsilon_{xy}(\bar{\omega}) \end{Bmatrix} \quad (17)$$

In the equation (17), the shear-extension coupling terms ( $A_{16}$  &  $A_{26}$ ) vanish for the considered

$[\pm\theta_m/90_n]_s$  family of the composites and then above equation can be written as,

$$\begin{Bmatrix} \varepsilon_x(\bar{\omega}) \\ \varepsilon_y(\bar{\omega}) \\ \varepsilon_{xy}(\bar{\omega}) \end{Bmatrix} = \begin{bmatrix} \dot{a}_{11}(\bar{\omega}) & \dot{a}_{12}(\bar{\omega}) & \dot{a}_{16}(\bar{\omega}) \\ \dot{a}_{12}(\bar{\omega}) & \dot{a}_{22}(\bar{\omega}) & \dot{a}_{26}(\bar{\omega}) \\ \dot{a}_{16}(\bar{\omega}) & \dot{a}_{26}(\bar{\omega}) & \dot{a}_{66}(\bar{\omega}) \end{bmatrix} \begin{Bmatrix} N_x(\bar{\omega}) \\ N_y(\bar{\omega}) \\ N_{xy}(\bar{\omega}) \end{Bmatrix} \quad (18)$$

The term  $\dot{a}_{11}$  includes the shear effect due to layer stiffness transformation and the term  $\dot{a}_{16}$  and  $\dot{a}_{26}$  will be zero for the equation (18). Polyzois *et al.* [26] derived an equation for calculating the effective longitudinal modulus ( $E_{eff}$ ) as,

$$E_{eff}(\bar{\omega}) = \frac{1}{\dot{a}_{11}(\bar{\omega})t(\bar{\omega})} \quad (19)$$

For structural elements where wall thickness is much smaller than the beam dimension, the rigidity of the beam is dependent minimally on the local rigidity of the wall. Estivalezes and Barrau [28] described that for the thin walled cross section of a beam structure, the local rigidities can be neglected, i.e. the thin walled beam can be analyzed by using only the external stiffness matrix. Ferrero [27] discussed the applicability of external stiffness matrix to analyze such structures on the basis of equideformability hypothesis. Therefore, effective modulus ( $E_{eff}$ ) can be used for both axial and flexural characteristics to model the appropriate structural behavior of the member. In this context, it can be noted that the probable location of matrix cracking damage may depend on the intended operation of the structural member during its service life. For example, cracks should appear at the top and bottom portion of a beam for the applications where only vertical loads (such as gravity induced loads) are applied. However, the present paper is intended to show a generalized situation where loads may act from any direction (such as the shaft of a wind turbine, transmission poles, tail boom of helicopter or tube like structures in missiles, submarine hulls etc.), wherein cracks may appear at any location of the beam throughout the cross-section. For this reason, the matrix cracking damage has been considered throughout the beam section with randomly varying crack density along length. However, as a special case, damage can be modeled only at the top and bottom portions of the beam following the proposed SRVE approach (refer to section 4.1) for a specific application.

The composite beam structures are considered as one dimensional Euler-Bernoulli cantilever beam with the following governing equation,

$$\frac{\partial^2}{\partial x^2} \left[ E_{eff}(\bar{\omega}) \{I(x)\}(\bar{\omega}) \frac{\partial^2 w(\bar{\omega})}{\partial x^2} \right] + \{m(x)\}(\bar{\omega}) \frac{\partial^2 w(\bar{\omega})}{\partial t^2} = 0 \quad (20)$$

where,  $E_{eff}$  can be obtained from Equation (19) and cross-sectional area ( $A$ ) can be computed as  $A = 2\pi R t$  and moment of inertia as  $I = \pi R^3 t$  (considering  $R \equiv R_2 \approx R_1$  for thin walled section, where  $R_1$  and  $R_2$  are the outer and inner radius of the hollow circular section) for a hollow cantilever circular composite beam [26]. For calculating the natural frequency of a non-uniform beam having spatially random variation of material properties as well as the matrix cracking, an approximate finite element method is used [29]. From the stiffness and mass matrices of a finite number of elements, the global stiffness matrix  $K_g$  and the global mass matrix  $M_g$  are obtained and thereby the following eigenvalue problem is solved for natural frequencies

$$K_g(\bar{\omega})\varphi = \omega^2 M_g(\bar{\omega})\varphi \quad (21)$$

From the above numerical equation, the natural frequency  $\omega$  and the Eigen vector ( $\varphi$ ) can be obtained for a beam having spatially random variation of material properties and matrix cracking damage. In this context, the necessity of adopting a finite element based approach instead of well-established analytical solutions for circular beam can be noted. The present study deals with a stochastic system having spatially varying structural and material attributes. It is true that analytical solutions are available for a beam-like structure and they are computationally efficient. But the major drawback of such analytical approaches is that they cannot account for the effect of spatially varying system properties. For this reason finite element analysis coupled with the SRVE approach is implemented in the present study. However, finite element analyses are generally time consuming and computationally intensive (especially in a stochastic framework where thousands of simulations are needed to be carried

out). To mitigate this lacuna a radial basis function based approach is proposed. Thus considering the present problem of spatially varying system attributes, the most effective way of analysis is surrogate based finite element analysis, as followed in this study.

### 3. Radial Basis Function (RBF)

Recent engineering designs and analyses use approximation of costly objective functions (i.e. expensive simulations/experiments) where surrogate models are being used to save significant costs by substituting some of the numerical simulations and experimental analysis which are necessary to achieve an optimal solution (refer figure 3). Surrogate models can reduce the high costs and extensive time demands which are needed for evaluations and also reduce the number of evaluations for any design estimation. In the present analysis MCS has been adopted for probabilistic characterization of natural frequencies that involves thousands of realizations to be performed. Generally for complex composite structures, the performance functions/ output quantities of interest (natural frequency in the present study) are not available as an explicit mathematical function of the stochastic input variables. Thus, the stochastic responses of the composite structure can only be evaluated numerically by following a structural analysis procedure (finite element analysis) which is often computationally quite intensive. The situation gets even more aggravated in the present problem due to consideration of matrix cracking damage in composites that necessitates a multi-step procedure to be carried out in order to obtain the final outputs. The RBF model is employed in this study to construct a predictive and representative surrogate of the actual model relating the natural frequencies to a number of stochastic input parameters. The RBF model is capable of obtaining results of the structural analysis encompassing every possible combination of all input variables.

A surrogate model distinguishes a relation among a vector of  $d$  real valued input variables (features),  $x = (x_1, x_2, \dots, x_d)$  and a single real valued output variable  $y$ . Using a

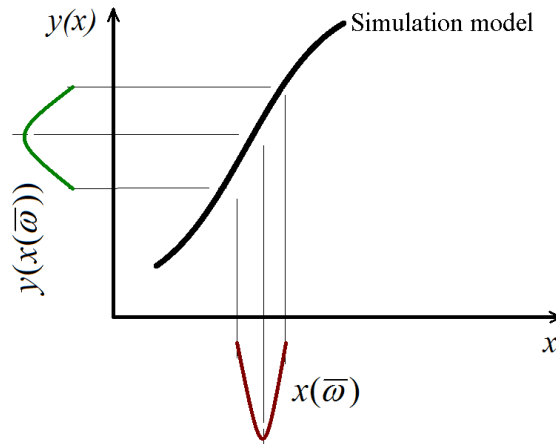


**Fig. 3** Description of the system showing stochastic input parameters ( $x(\bar{\omega})$ ) and output response ( $y(x(\bar{\omega}))$ ). The original simulation model has been replaced by RBF model to achieve computational efficiency in the present study.

finite number  $n$  of training observations (data cases or data points)  $(x_{(i)}, y_{(i)})$ ,  $i = 1, 2, \dots, n$  the objective is to establish a model  $F$  that permits predicting the output value for yet unseen input parameter sets as closely as possible. The radial basis function method was first used by Hardy [22] for the interpolation of geographical scattered data and later used by Kansa [30] for the solution of partial differential equation. Radial basis functions (RBF) were mainly developed for scattered multivariate data interpolation which uses a series of basic functions that are centrally symmetric at each sampling point [22]. RBF functions are special class of functions with main characteristic being that their responses increase or decrease monotonically from the central point with distance [31]. Quadratic surrogates have the benefit of being easy to implement while still being able to model curvature of the underlying function. Another way to model curvature is to consider interpolating surrogates, which are linear combinations of nonlinear basis functions and satisfy the interpolation points. RBF is often used to perform the interpolation of scattered multivariate data [32-34]. The use of RBF models for two dimensional solids was proposed by Liu *et. al.* [35] and incorporated to isotropic and composites plates by Ferreira and Fasshauer [36]. Detailed review on RBF methods can be found in the scientific literatures [37-41].

The RBF model depends only upon the distance to a centre point  $x_j$  and is of the form  $g(\|x-x_j\|)$  and RBF may also depend on the shape parameter called  $c$ , in which case  $g(\|x-x_j\|)$  may be replaced by  $g(\|x-x_j, c\|)$  [39-43, 30]. Considering a set of nodes  $x_1, x_2, \dots, x_N \in \Omega \subset R^n$ , the radial basis functions centred at  $x_j$  are expressed as

$$g_j(x) \equiv g(\|x-x_j\|) \in R^n, j = 1, \dots, N \quad (22)$$

where,  $\|x-x_j\|$  is the Euclidian norm. The radial function for RBF model can be expressed as,

$$g_j(x) \equiv e^{-c^2\|x-x_j\|^2} \quad (\text{For Gaussian}) \quad (23)$$

$$g_j(x) \equiv (\|x-x_j\| + c^2)^{\frac{1}{2}} \quad (\text{For multi-quadratic}) \quad (24)$$

$$g_j(x) \equiv (\|x-x_j\| + c^2)^{-\frac{1}{2}} \quad (\text{For inverse multi-quadratic}) \quad (25)$$

$$g_j(x) \equiv \|x-x_j\|^2 \log\|x-x_j\| \quad (\text{For Thin plate splines}) \quad (26)$$

$$g_j(x) \equiv \|x-x_j\|^k, k = 1, 3, 5, \dots \quad (\text{For Biharmonic}) \quad (27)$$

$$g_j(x) \equiv \|x-x_j\|^k \log\|x-x_j\|, k = 2, 4, 6, \dots$$

where  $c$  is a shape parameter. RBFs are insensitive to spatial dimension, making the implementation of the method much easier than the finite element analysis [37-40]. However, such an interpolation method has shortcomings in that the appearance of a meta-model varies significantly with the type of basis function and its internal parameters. An important characteristic of radial basis function is that it does not require any kind of grid and the only geometric property needed for RBFs are the pairwise distances between points. Working with higher dimensional problems by using RBF models are not difficult as the distances are easy to compute in any number of space dimensions. In the present study, the basis function has been chosen by comparing relative performance with respect to original Monte Carlo simulation and the RBF has been employed with the fixed parameter  $c^2 = 1$ . The accuracy of the results may

depend on the shape parameter  $c$ . It should be noted that an RBF passes through all the sampling points exactly. This means that function values from the approximate function are equal to the true function values at the sampling points. This can be seen from the way that the coefficients are found. The local deviation at an unknown point ( $x$ ) is explicated using stochastic processes. In the present study, the performance of the RBF models have been verified and validated with respect to original Monte Carlo simulation. In the next section the proposed RBF based stochastic analysis algorithm is discussed including the effect of noise.

#### **4. Stochastic representative volume element (SRVE) approach coupled with RBF**

##### ***4.1. Concept of SRVE***

In this article a novel concept of stochastic representative volume element (SRVE) has been proposed to account for the spatially random variation of material properties and crack density. In this approach, each representative unit (structural elements) of the structure are considered as stochastic, instead of considering homogenized properties of a conventional representative volume element (RVE) throughout the entire domain. In traditional approach, typically one RVE is considered for the purpose of the analysis. It is assumed that a single RVE represents the entire analysis domain [1]. However, this way of analysis may often lead to erroneous results, specially for stochastic systems having spatially random variation of material and other attributes. For analyzing such systems, it is necessary to take into account the stochastic structural attributes along the spatial location of different zones.

In the present approach of analysis, the entire structure is considered to be consisted of a finite number of such SRVEs. Thus, properties of each SRVE are the functions of its stochastic material properties and crack density. Following this approach, it becomes feasible to account for the spatial variability in a structural system in a more realistic manner. The global properties (such as natural frequencies) of the structure are obtained by propagating the structural informations acquired in the elementary level (SRVEs) towards the global level through

assembling the SRVEs using principles of mechanics (finite element approach in the present study). Similar concept has been put forth recently for analyzing hexagonal lattices with spatial irregularity [44-45], wherein representative unit cell elements (RUCE) were considered instead of the conventional unit cells. The entire lattice was considered to be consisting of several such RUCEs and the global properties of the entire irregular lattice is obtained by assembling the RUCEs following equilibrium and compatibility conditions. In this article, we have generalized the idea of RUCE for stochastic analysis of a beam like structure in the form of SRVE. The consideration of SRVE in a beam like structure shows in the Figure 4, wherein the beam is divided into a finite number of SRVEs having a length of  $x$  each. Thus each of such SRVEs have different material properties and crack density. A parameter stochastic characteristic length ( $r$ ) is defined as:  $r = \frac{x}{L} = \frac{1}{N_d}$ , where  $N_d$  is the number of divisions along the length of the beam.

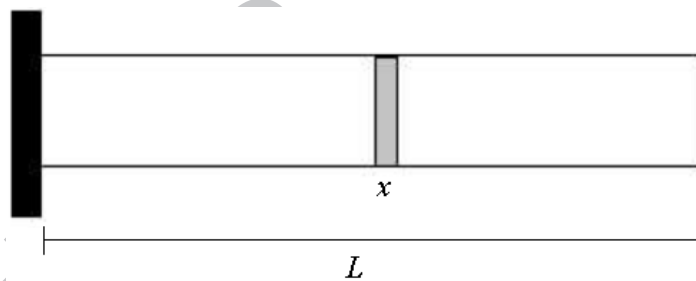


**Fig. 4** Consideration of SRVE for analyzing the spatially random system (Cantilever beam with varying structural attributes along the length)

#### **4.2. RBF based algorithm for stochastic analysis of thin-walled composite beam**

The stochasticity in material properties of laminated composite circular thin walled beams, such as longitudinal elastic modulus, transverse elastic modulus, shear modulus, Poisson's ratio, mass density and geometric properties such as ply-orientation angle are considered as input parameters for analysis of natural frequencies. It is presumed that the distribution of randomness of input parameters exists within a certain band of tolerance

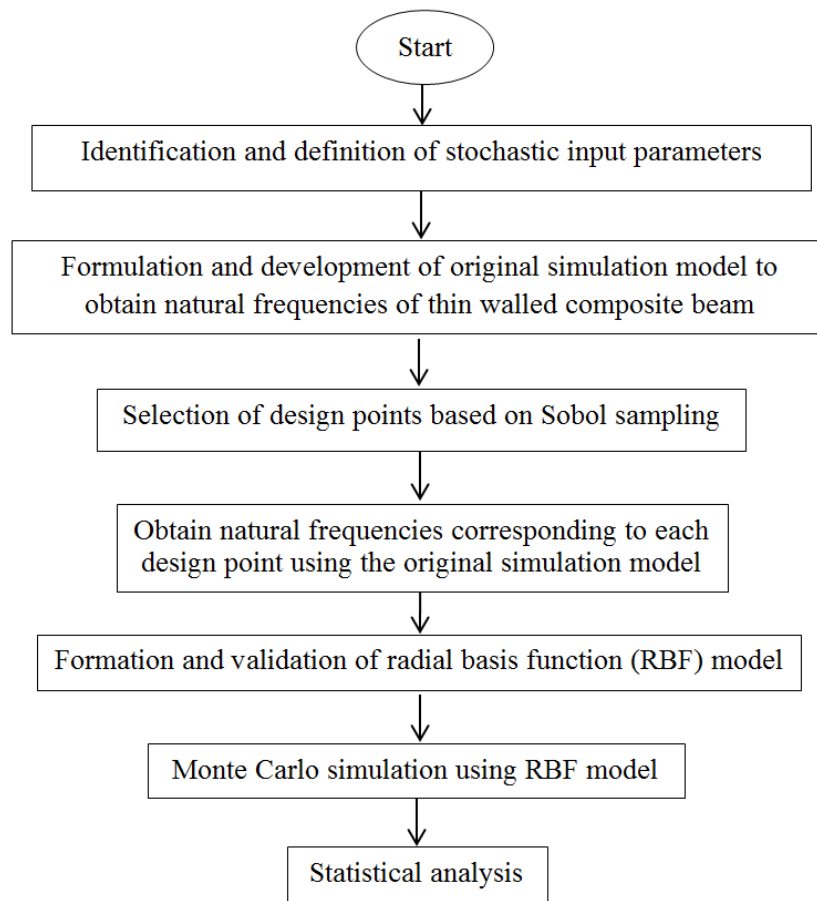


**Fig. 5** Flowchart for stochastic natural frequency analysis based on RBF model

following random uniform distribution with the central deterministic mean values. A variation of  $\pm 10\%$  from deterministic value for material properties and fibre orientation angle is assumed for the purpose of analyses following industry standards, unless otherwise mentioned. The percentage variation is regarded as the degree of stochasticity ( $\Delta$ ). In the present study, two separate analyses have been carried out considering the stochasticity in micro-mechanical properties and the stochasticity in macro-mechanical properties to understand the cascading effect of stochasticity on a comparative basis. Thus the following two cases of stochasticity are considered for material properties:

- (i) Combined variation for macro-mechanical properties of elastic moduli, shear moduli, Poisson's ratio and mass density can be written as,

$$g_{macro} \{E_1(\bar{\omega}), E_2(\bar{\omega}), G_{12}(\bar{\omega}), G_{13}(\bar{\omega}), G_{23}(\bar{\omega}), \mu(\bar{\omega}), \rho(\bar{\omega})\}$$

$$= \left\{ \begin{array}{l} \phi_{macro}^1(E_{1(1)} \dots E_{1(l)}), \phi_{macro}^2(E_{2(1)} \dots E_{2(l)}), \phi_{macro}^3(G_{12(1)} \dots G_{12(l)}), \phi_{macro}^4(G_{13(1)} \dots G_{13(l)}), \\ \phi_{macro}^5(G_{23(1)} \dots G_{23(l)}), \phi_{macro}^6(\mu_{(1)} \dots \mu_{(l)}), \phi_{macro}^7(\rho_{(1)} \dots \rho_{(l)}) \end{array} \right\}$$

(ii) Combined variation for micro-mechanical properties of elastic moduli (fibre and matrix), shear moduli (fibre and matrix), Poisson ratios (fibre and matrix), mass densities (fibre and matrix) and volume fraction can be written as,

$$g_{micro} \{E_{1f}(\bar{\omega}), E_{2f}(\bar{\omega}), E_m(\bar{\omega}), G_f(\bar{\omega}), G_m(\bar{\omega}), \mu_f(\bar{\omega}), \mu_m(\bar{\omega}), \rho_f(\bar{\omega}), \rho_m(\bar{\omega}), V_f(\bar{\omega})\}$$

$$= \left\{ \begin{array}{l} \phi_{micro}^1(E_{1f(1)} \dots E_{1f(l)}), \phi_{micro}^2(E_{2f(1)} \dots E_{2f(l)}), \phi_{micro}^3(E_{m(1)} \dots E_{m(l)}), \phi_{micro}^4(G_{f(1)} \dots G_{f(l)}), \phi_{micro}^5(G_{m(1)} \dots G_{m(l)}), \\ \phi_{micro}^6(\mu_{f(1)} \dots \mu_{f(l)}), \phi_{micro}^7(\mu_{m(1)} \dots \mu_{m(l)}), \phi_{micro}^8(\rho_{f(1)} \dots \rho_{f(l)}), \phi_{micro}^9(\rho_{m(1)} \dots \rho_{m(l)}), \phi_{micro}^{10}(V_{f(1)} \dots V_{f(l)}) \end{array} \right\}$$

where,  $E_{1(i)}$ ,  $E_{2(i)}$ ,  $G_{12(i)}$ ,  $G_{13(i)}$ ,  $G_{23(i)}$ ,  $\mu_i$ ,  $\rho_i$  are the longitudinal elastic modulus, transverse elastic modulus, shear modulus in three different planes, Poisson's ratio and mass density of  $i^{th}$  layer, respectively and  $l$  denotes the number of layers in the laminate. For the stochasticity in micro-mechanical properties,  $E_{1f(i)}$ ,  $E_{2f(i)}$ ,  $E_{m(i)}$ ,  $G_{f(i)}$ ,  $G_{m(i)}$ ,  $\mu_{f(i)}$ ,  $\mu_{m(i)}$ ,  $\rho_{f(i)}$ ,  $\rho_{m(i)}$ ,  $V_{f(i)}$  denote elastic moduli of fibre in longitudinal and transverse direction, elastic modulus of matrix, shear modulus of fibre and matrix, Poisson's ratio of fibre and matrix, mass density of fibre and matrix and volume fraction corresponding to  $i^{th}$  layer, respectively. In addition to the above mentioned cases of material property variation, matrix cracking has been considered in a stochastic framework to analyse the natural frequencies of the structure.

To achieve computational efficiency, an RBF based uncertainty quantification algorithm has been developed as presented in figure 5. For constructing the RBF surrogate model, both Latin hypercube sampling [46] and Sobol sequence [47] have been studied to assess their comparative performance. In this surrogate based approach, first the surrogate model (RBF) is formed on the basis of few optimally chosen design points. Thus same number (number of design points) of finite element simulation/ experiments is needed to be carried out at this stage. The RBF model effectively replaces the actual expensive finite element model by an efficient mathematical model. Once the surrogate model is formed, thousands of virtual simulations can

be carried out for different random combinations of input parameters using the computationally efficient RBF model.

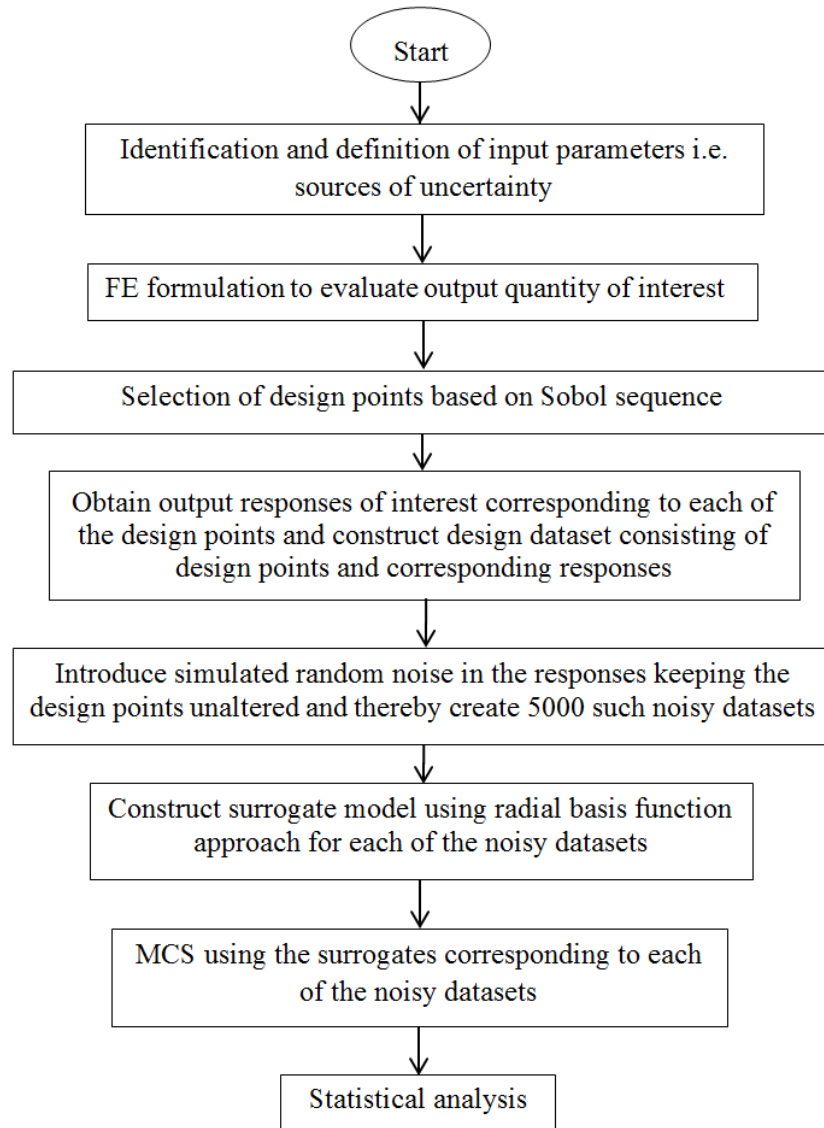


**Fig. 6** Flowchart for analyzing the effect of noise on uncertainty quantification algorithm based on RBF model

#### 4.3. Effect of noise on RBF based stochastic analysis algorithm

The effect of noise on the proposed RBF based stochastic analysis algorithm is accounted by incorporating different levels of Gaussian noise as shown in figure 6. A Gaussian white noise with a specific factor ( $p$ ) is introduced in the set of output responses, which is used subsequently for the RBF model formation, as

$$f_{ijN_s} = f_{ij} + p \times \xi_{ij} \quad (28)$$

Here,  $f$  represents natural frequency and the subscript  $i$  and  $j$  denote frequency number and sample number respectively;  $\xi_{ij}$  is a function which generates random numbers with normal distribution having zero mean and unit standard deviation and  $p$  (noise level) in the equation (28) basically represents the standard deviation corresponding to the noise level. The subscript  $N_s$  is used here to indicate the noisy frequency.

Thus the simulated noisy set of data (i.e. the sampling matrix for RBF model formation) is constructed by incorporating pseudo random noise in the responses (natural frequencies), while the input design points are allowed to remain unaltered. Subsequently for each of the datasets, RBF based Monte Carlo simulation is performed to quantify uncertainty in the thin walled composite beam. Effect of noise has been analysed following a deterministic approach in several other studies [48-51]. Assessment of the effect of noise on RBF based uncertainty propagation algorithm is investigated for the first time in this study. Such simulated noise can be considered as accounting other sources of uncertainty such as error in computer modelling, error in measurement and various other forms epistemic uncertainties inherently involved with the structural system. Thus the present approach of considering noise in uncertainty analysis will provide a comprehensive idea regarding the robustness of RBF based algorithm under noisy data.

## 5. Results and discussion

In this article, results have been presented for two different classes of stochasticity: randomly homogeneous system and randomly inhomogeneous system. In randomly homogeneous system, no spatial variability along the length of the beam is considered. It is assumed that structural attributes remain same spatially. However the stochastic parameters vary from sample to sample following a probabilistic distribution (random variable approach). In

**Table 1:** Deterministic micromechanical properties of composite [52]

Property	Value
Longitudinal modulus for fibre ( $E_{1f}$ )	80 GPa
Transverse modulus for fibre ( $E_{2f}$ )	80 GPa
Poisson's ratio for fibre ( $\mu_f$ )	0.2
Shear modulus for matrix ( $G_f$ )	33.33 GPa
Mass density for fibre ( $\rho_f$ )	2.55 gm/cc
Mass density for matrix ( $\rho_m$ )	1.265 gm/cc
Elastic modulus of matrix ( $E_m$ )	4.2 GPa
Shear modulus for matrix ( $G_m$ )	1.567 GPa
Poisson's ratio for matrix ( $\mu_m$ )	0.34
Fibre volume fraction ( $V_f$ )	0.61

**Table 2:** Deterministic macro-mechanical properties for  $V_f = 0.61$ 

Property	Value
Longitudinal modulus ( $E_1$ )	48 GPa
Transverse modulus ( $E_2$ )	13.3 GPa
Poisson's ratio ( $\mu_{12}$ )	0.235
In-plane shear modulus ( $G_{12}$ )	5.17 GPa
Mass density ( $\rho$ )	1.94 gm/cc
Shear modulus ( $G_{13}$ )	5.17 GPa
Transverse shear modulus ( $G_{23}$ )	4.12 GPa

randomly inhomogeneous system, spatial variability of the stochastic structural attributes are accounted. Thus, in this form of stochasticity the material and damage parameters vary randomly along the length as well as vary from sample to sample. For the purpose of obtaining numerical results, a long circular cross section of a composite beam is considered in the present analysis having a length of  $18\text{ m}$ , outer diameter of the circular cross section as  $600\text{ mm}$  and the beam wall cross-section as  $11\text{ mm}$  [26]. The  $[\pm\theta_m/90_n]_s$  configuration of laminate is considered for the analyses similar to Nuismer and Tan [24]. The deterministic micromechanical material properties (E-glass 21xK43 Gevetex/ 3501–6 epoxy) of the composite beam are presented in Table 1 [52]. Using Halpin- Tsai principle [25] the deterministic macromechanical properties are calculated by considering a volume fraction ( $V_f$ ) of 0.61 and presented in Table 2. Results in this article has been shown for two different cases (stochasticity in micromechanical properties:  $g_{micro}$  and stochasticity in macromechanical properties:  $g_{macro}$ ) as discussed in section 4.2. Thus, for stochasticity in micromechanical properties, the material parameters presented in Table 1 are considered as stochastic and thereby the macromechanical properties are calculated using Halpin- Tsai principle to carry out further analysis including the effect of matrix cracking as shown in figure 12 (detailed discussion about this figure is provided later). For stochasticity in macro-mechanical properties, the analysis starts one step ahead in the hierarchy i.e. uncertainty is considered in the macro-mechanical material properties as shown in Table 2. Subsequently, the results have been compared to analyse the cascading effect in stochasticity.

### 5.1. Validation and convergence study

The deterministic finite element model of the thin-walled composite beam is validated with available literature before carrying out further analyses (refer to Table 3). The fundamental natural frequencies are compared with the results obtained by Polyzois *et al.* [26] for different laminate configurations of  $[\pm\theta_m]_s$  and  $m = 25$  family of composites. The number of elements in

the finite element model is based on a mesh convergence study showing that the results converge at eight number of elements for the undamaged structure. Another convergence study is performed for selection of sample size for Radial based function based surrogate that is compared to the baseline original MCS (10,000 samples) results considering macro and micro mechanical properties. Two different sampling techniques (Latin hypercube sampling and Sobol sequence) have been considered and their comparative performances are presented in Table 4 and Table 5 based on statistical analyses (with  $\theta = 30^\circ, m = 16, n = 18$  in  $[\pm\theta_m/90_n]_s$  family of composites). The adequate sample sizes for macro-mechanical and micro-mechanical analyses are found to be 128 and 256 respectively. It is also noticed that performance of Sobol sequence is better compared to LHS. Similar conclusion can be made from figure 7 that shows the absolute percentage error in different statistical parameters with respect to original MCS. Figure 8 presents typical results of probability density function plots for original MCS along with different sample sizes of Sobol sampling considering stochasticity in micro-mechanical properties. Another study has been carried out to assess the performance of different basis functions for the construction of RBF model as presented in figure 9. The figure reveals that performance of thin plate splines is slightly better than other basis functions. Thus the results presented in this article hereafter will consider Sobol sampling and thin plate splines.

**Table 3:** Validation of fundamental frequencies for the undamaged composite structure for typical fibre orientation angles ( $\theta$ ):

$\theta$	Fundamental natural frequencies (rad/ sec)	
	Present study	Polyzois <i>et al.</i> [26]
0°	11.45	11.35
15°	10.72	10.63
30°	8.61	8.55
45°	6.57	6.53

**Table 4:** Maximum value, minimum value, mean value and standard deviation of first three natural frequencies for  $\rho$  obtained using original MCS and RBF surrogate modelling considering different sample sizes for LHS and Sobol sampling

Natural Frequency		MCS	Sample size=32		Sample size=64		Sample size=128		Sample s
			LHS	Sobol	LHS	Sobol	LHS	Sobol	LHS
<b>Maximum</b>	First	8.2083	8.1272	8.1694	8.1563	8.1314	8.1669	8.1555	8.1730
	Second	51.4412	50.9329	51.1972	51.1151	50.9590	51.18164	8.1555	51.2199
	Third	144.0389	142.6156	143.3558	143.1259	142.6887	143.3121	143.1117	143.4193
<b>Minimum</b>	First	6.80513	6.8503	6.8326	6.8405	6.8236	6.7960	6.8207	6.8246
	Second	42.6471	42.9307	42.8195	42.8688	42.7632	42.5904	42.7448	42.7693
	Third	119.4148	120.2090	119.8976	120.0357	119.7401	119.2560	119.6886	119.7570
<b>Standard deviation</b>	First	0.2714	0.2626	0.2692	0.2695	0.2669	0.2732	0.27238	0.2711
	Second	1.7012	1.6462	1.6874	1.6893	1.6730	1.7123	1.7070	1.6995
	Third	4.76358	4.6095	4.7250	4.7304	4.6847	4.7946	4.7797	4.7588
<b>Mean</b>	First	77.4724	7.4689	7.4633	7.4674	7.4680	7.4671	7.4639	7.46961
	Second	46.8288	46.8073	46.7723	46.7979	46.8017	46.7961	46.7758	46.8113
	Third	131.1241	131.06378	130.9656	131.0375	131.0480	131.0324	130.97569	131.0751

**Table 5:** Maximum value, minimum value, mean value and standard deviation of first three natural frequencies for micro-m... using original MCS and RBF surrogate modelling considering different sample sizes for LHS and Sobol sampling

Natural Frequency		MCS	Sample size=32		Sample size=64		Sample size=128		Sample
			LHS	Sobol	LHS	Sobol	LHS	Sobol	LHS
<b>Maximum</b>	First	8.3027	8.2553	8.2385	8.3381	8.2987	8.2580	8.2556	8.2902
	Second	52.0328	51.7352	51.6303	52.2546	52.0076	51.7521	51.7374	51.9543
	Third	145.6955	144.8623	144.5685	146.3165	145.6250	144.9097	144.8683	145.4758
<b>Minimum</b>	First	6.67840	6.7663	6.7316	6.7509	6.74726	6.70267	6.7272	6.6804
	Second	41.8529	42.4038	42.1869	42.3074	42.2843	42.0050	42.1589	41.8654
	Third	117.1910	118.7336	118.1262	118.4637	118.3992	117.6170	118.0478	117.2261
<b>Standard deviation</b>	First	0.27660	0.2579	0.256	0.2655	0.26487	0.2704	0.26838	0.2725
	Second	1.7334	1.6162	1.6093	1.6643	1.6600	1.6948	1.6819	1.7083
	Third	4.8538	4.5255	4.5062	4.6603	4.6482	4.7457	4.7095	4.7834
<b>Average</b>	First	7.4651	7.4637	7.4687	7.4702	7.4669	7.4665	7.4639	7.4704
	Second	46.7835	46.7746	46.8056	46.8152	46.7945	46.7918	46.7759	46.8164
	Third	130.9971	130.9722	131.0590	131.0858	131.0279	131.0204	130.9759	131.0892

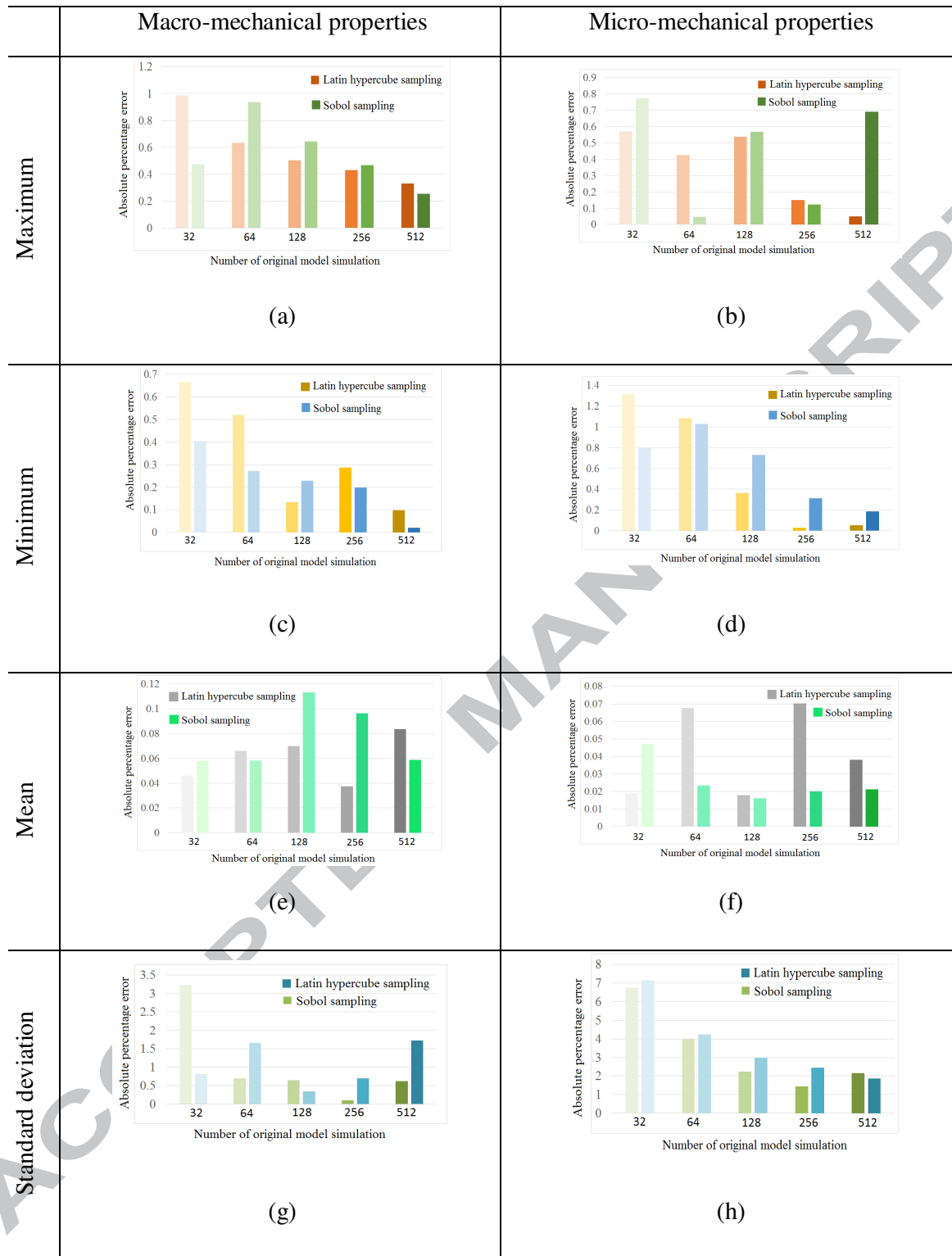


**Fig. 7** Absolute percentage error in maximum, minimum, mean and standard deviation of fundamental natural frequencies with respect to original MCS for micro and macro mechanical properties obtained for different sample sizes considering LHS and Sobol sampling.

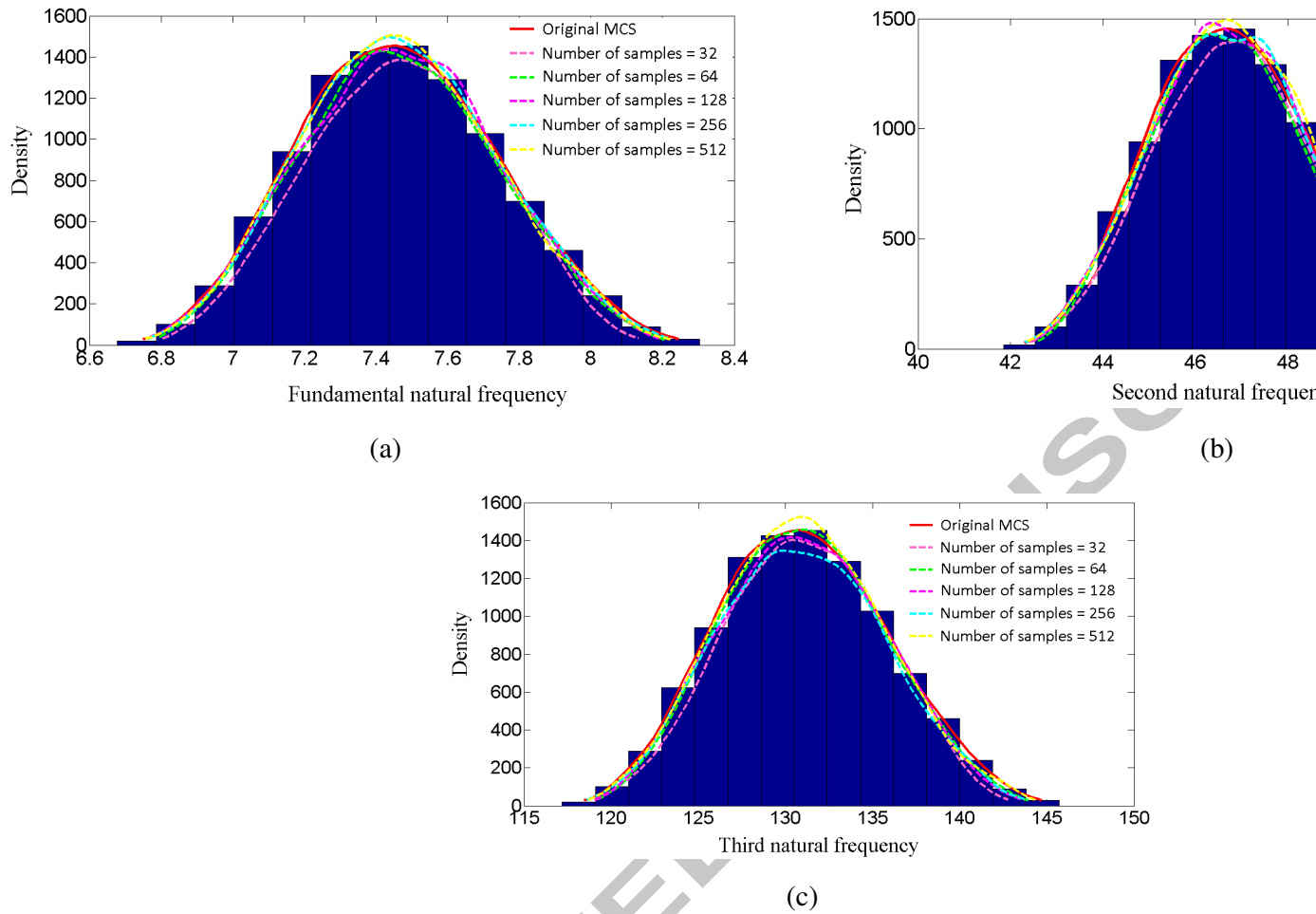
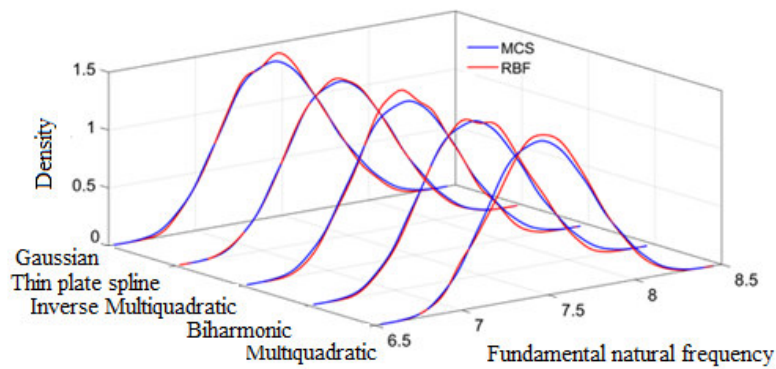
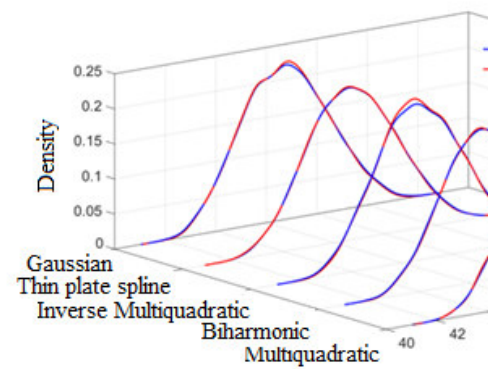


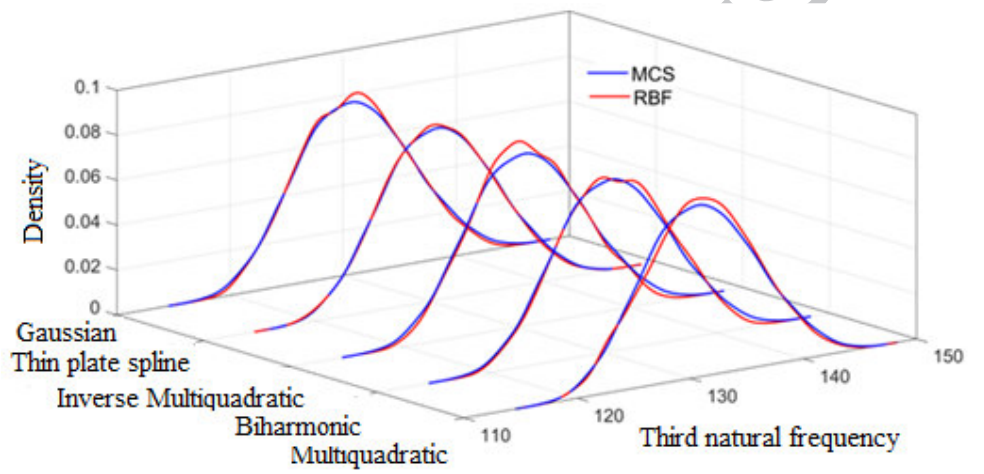
**Fig. 8** Probability density function plots for different sample sizes of Sobol sampling considering stochasticity in along with original MCS



(a)



(b)



(c)

**Fig. 9** Performance of different basis functions for constructing RBF model corresponding to first three n

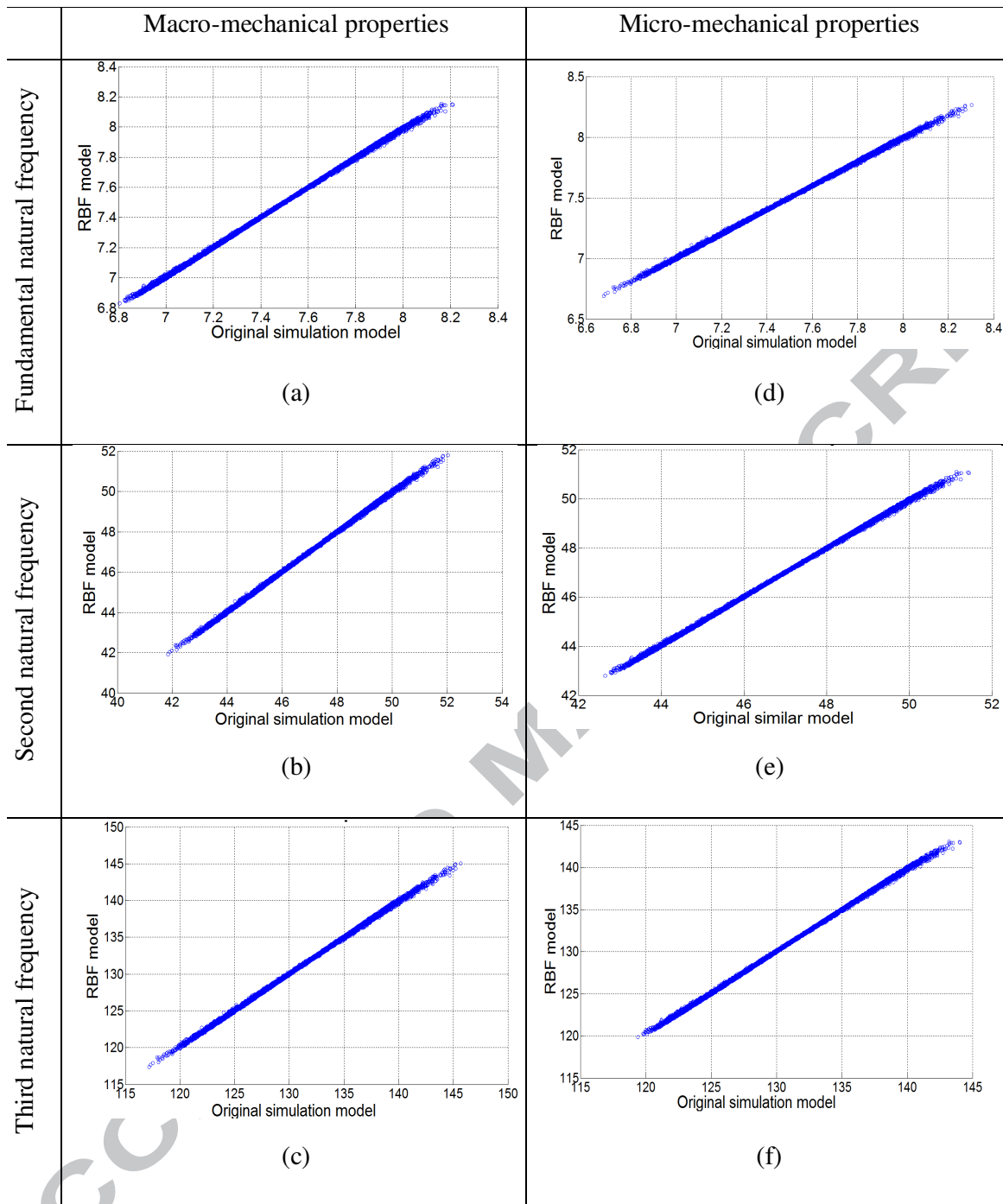


**Fig. 10** (a-c) Scatter plot of macro-mechanical properties obtained by original MCS and RBF model with respect to first three natural frequencies for circular thin walled composite beam, considering sample size=10000, with  $\theta = 30^\circ, m = 16, n = 18$ ; (d-f) Scatter plot of micro-mechanical properties obtained by original MCS and RBF model with respect to first three natural frequencies for circular thin walled composite beam, considering sample size =10000, with  $\theta = 30^\circ, m = 16, n = 18$

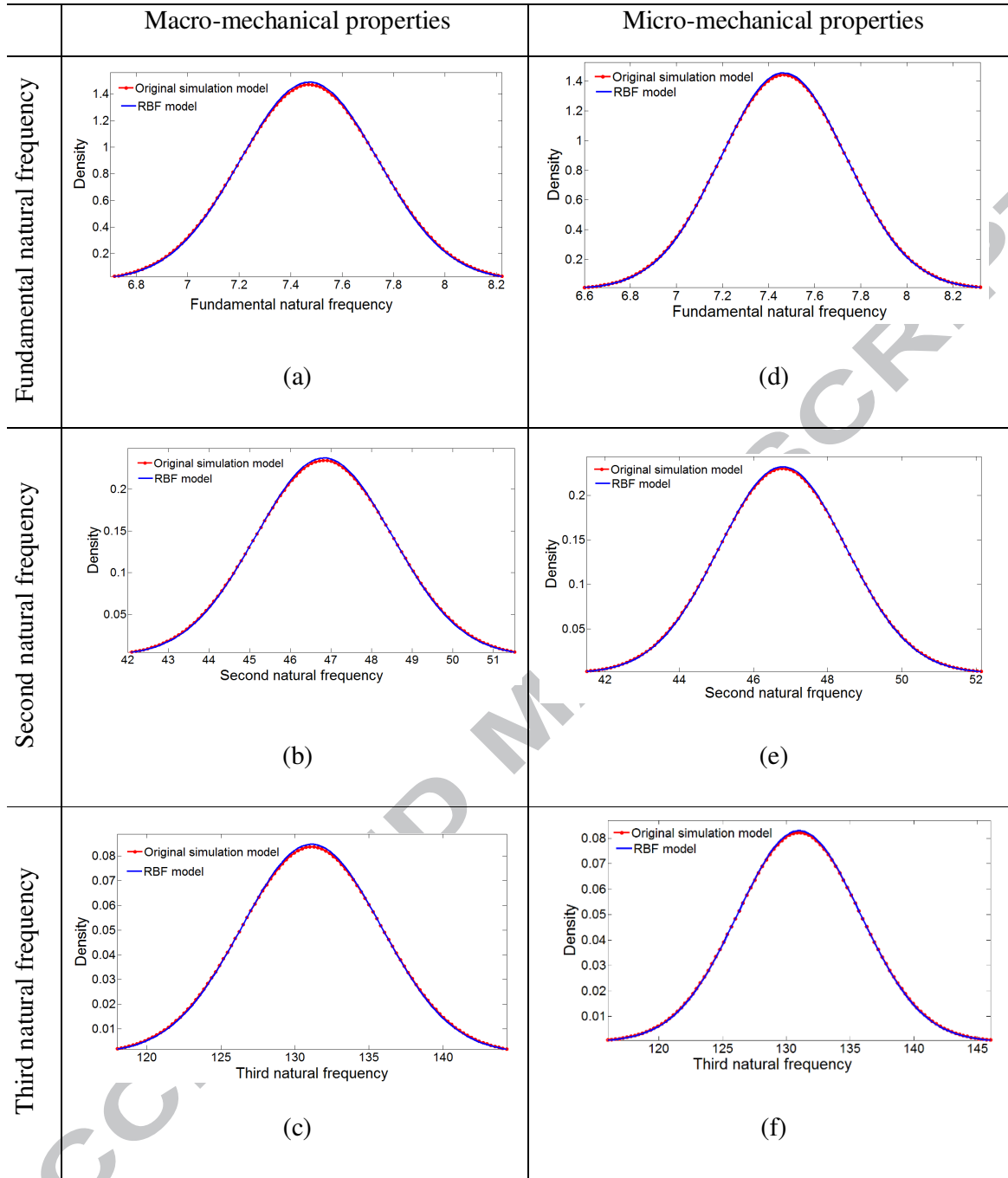
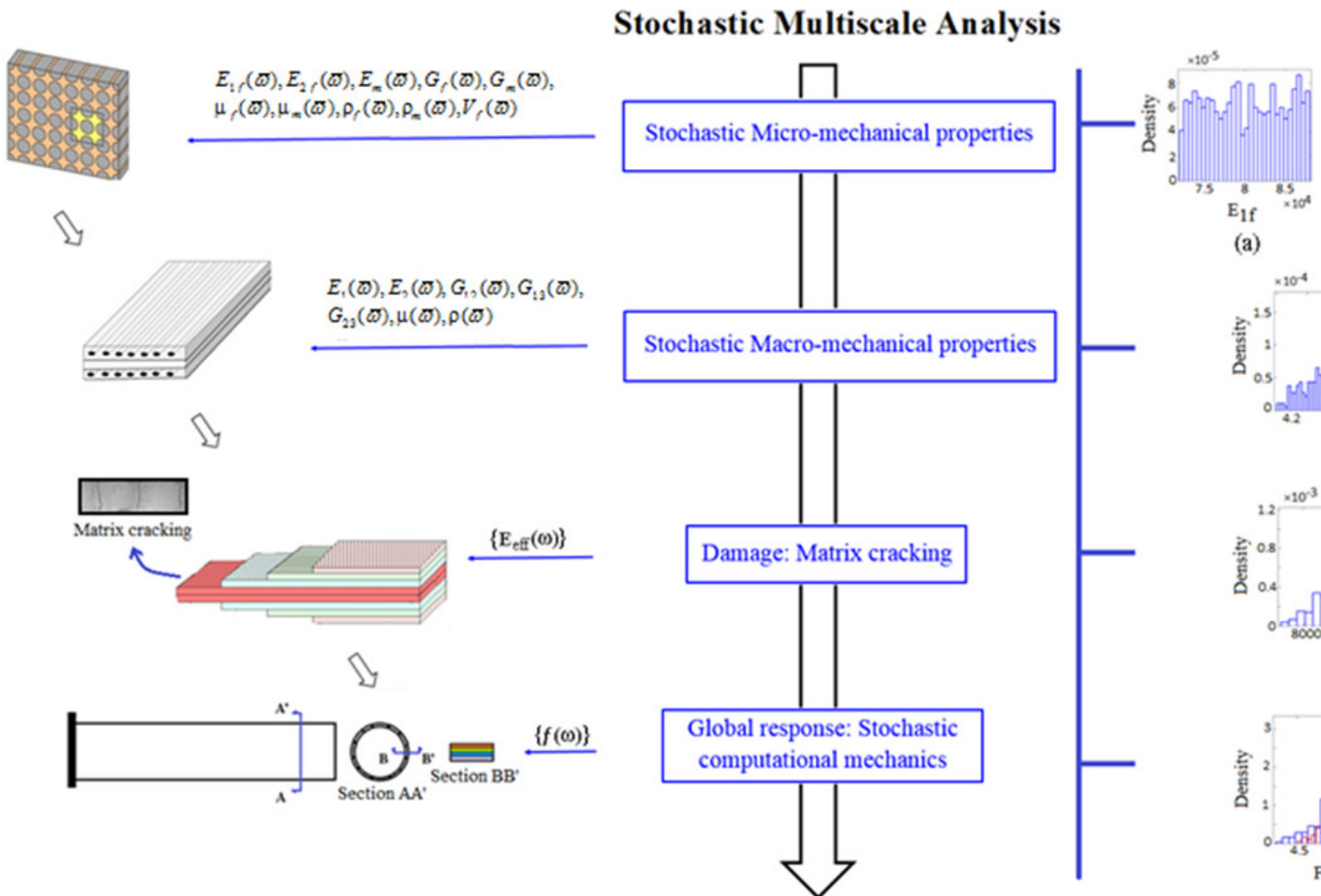


**Fig. 11** (a-c) Probability density function of macro-mechanical properties obtained by original MCS and RBF model with respect to first three natural frequencies for circular thin walled composite beam, considering sample size=10000, with  $\theta = 30^\circ, m = 16, n = 18$ ; (d-f) Probability density function of micro-mechanical properties obtained by original MCS and RBF model with respect to first three natural frequencies for circular thin walled composite beam, considering sample size = 10000, with  $\theta = 30^\circ, m = 16, n = 18$

Figure 10 and figure 11 show the scatter plots and probability density function plots for the converged sample sizes with respect to original MCS. The low scatterness of the points around the diagonal line in figure 10 and the low deviation between the probability density function estimations of original MCS and RBF model in figure 11 corroborate the fact that RBF surrogate models are accurately formed. It is worthy to mention here that by adopting the surrogate based approach, significant computational efficiency is achieved. Although same sampling size as in direct MCS (with sample size of 10,000) is considered in the present RBF based approach, the number of actual FE analysis is much less compared to original MCS and is equal to the number of representative samples required to construct the RBF meta-model. Hence, the computational time and effort expressed in terms of FE simulations is reduced significantly compared to full-scale direct MCS.

## 5.2. Results of stochastic analyses and discussion

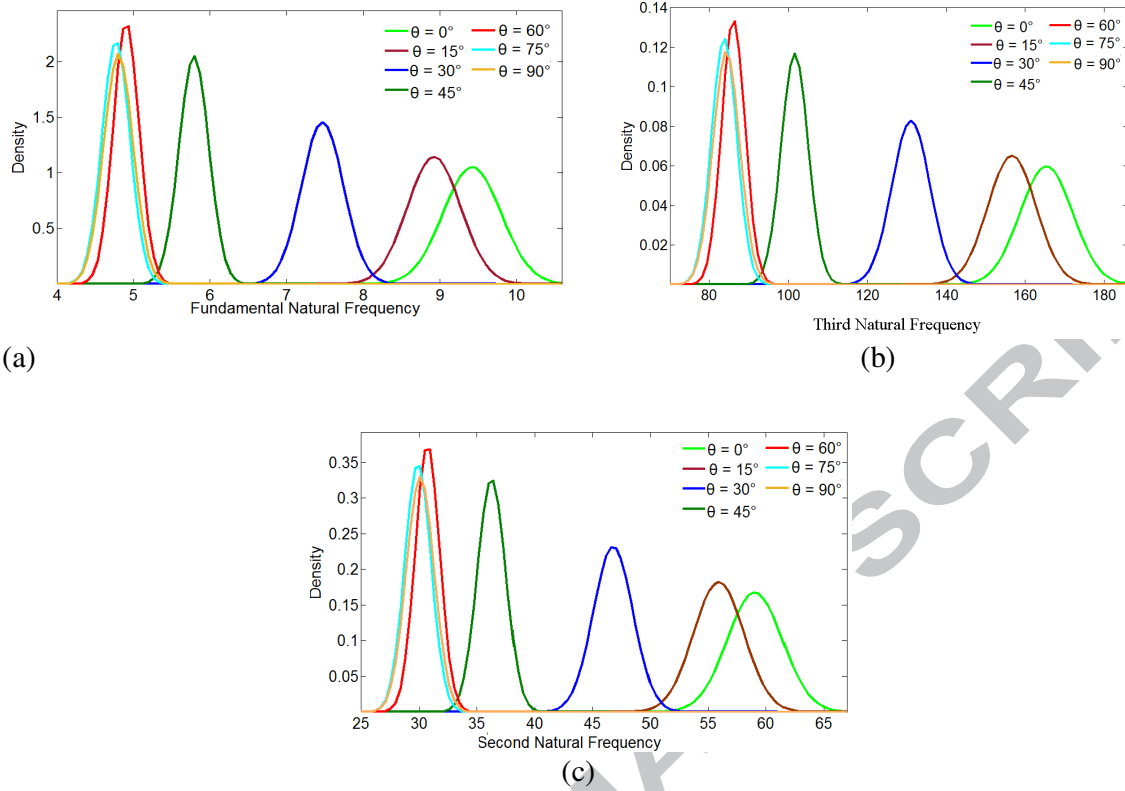
The stochastic multi-scale analysis that has been carried out in this study is depicted in figure 12 along with some representative results to elucidate the context of the present numerical investigation. Two different analyses for stochastic micro and macro mechanical properties ( $g_{micro}$  and  $g_{macro}$ ) are shown using appropriate colours to compare the probabilistic distributions in the global responses due to same degree of stochasticity in micro and macro-mechanical properties. The typical input distribution (uniform random) depicts in figure 12(a-c) for  $E_{1m}$ ,  $E_{1f}$  and  $V_f$  respectively (other micromechanical properties also follow the same distribution). In figure 12(d), two distributions are shown for  $E_1$ . The distribution depicted in blue colour corresponds to the macro-mechanical properties obtained from the stochastic micro mechanical properties (i.e. typical figure 12(a-c) and similar distributions of other stochastic micro-mechanical properties) by using the Halpin-Tsai principle [25]. The distribution depicted by red colour in figure 12(d) represents the typical input distribution (random uniform) of



**Fig. 12** Proposed stochastic multiscale analysis scheme of laminate composite beam with matrix cracking (In figures, blue and red colour indicate micro-mechanical and macro-mechanical properties respectively)

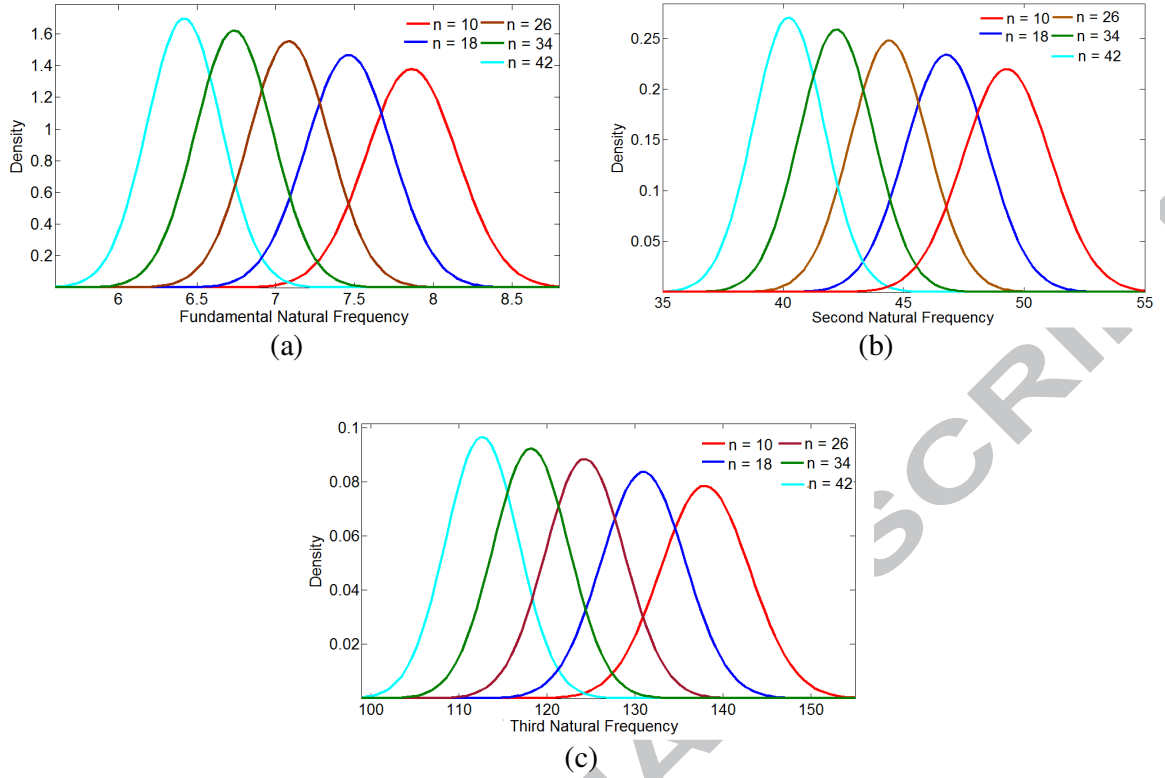
macro-mechanical analysis (other macro-mechanical properties follow similar distributions). It is noteworthy that, even though all the input distributions of micro-mechanical analysis (figure 12(d)) are uniform, the distributions of macro-mechanical properties obtained from the stochastic micro-mechanical properties appeared Gaussian. This observation can be explained by central limit theorem [53]. The typical distributions for  $E_{eff}$  (after incorporation of the effect of matrix cracking) and fundamental natural frequency showed in figures 12(e-f). In both the cases it can be noticed that response bound is more for micro-mechanical analysis compared to macro-mechanical analysis while same degree of stochasticity ( $\pm 10\%$  variation from deterministic value following uniform distribution) is considered in both the cases. This observation can be explained by the cascading effect showing that consideration of stochasticity in more elementary level of the multi-scale hierarchy increases the response bound of output parameters at the global level.

In this section, the probabilistic descriptions for first three natural frequencies are analysed for various structural configurations and matrix crack densities in the considered  $[\pm\theta_m/90_n]_s$  family of composites. Results presented in figure 13-18 have been obtained considering a randomly homogeneous system. In the figure 13, the probability density function plots for first three natural frequencies due to combined variation of stochastic input parameters are presented for  $\theta = 0^\circ, 15^\circ, 30^\circ, 45^\circ, 60^\circ, 75^\circ, 90^\circ$  considering  $m = 16, n = 18$ . A general tendency is observed that the mean and standard deviation of natural frequencies decrease with the increase of  $\theta$ . The reduction in the first three natural frequencies is due to reduction in longitudinal stiffness with increasing value of  $\theta$ . The probability density function plots are presented in figure 14 and figure 15 with respect to first three natural frequencies for different number of layers considering a fibre orientation angle  $\theta = 30^\circ$ . It is interesting to notice that with the increase in number of plies having  $90^\circ$  fiber orientation angle ( $n$ ), mean and standard deviation decrease (figure 14), while a reverse trend is found for number of plies having ply



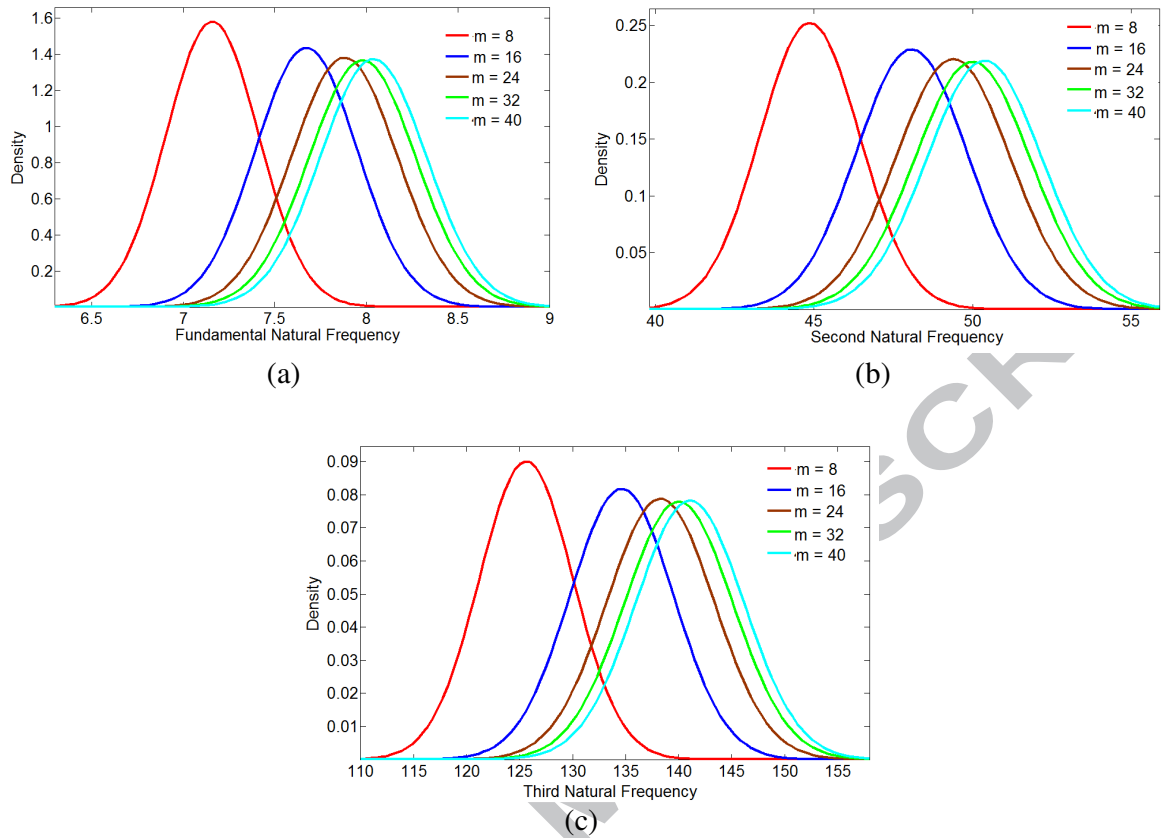
**Fig. 13** (a-c) Probability density function plots for first three natural frequencies for different fiber orientation angle ( $\theta$ )

orientation angle  $\theta = 30^\circ$  (figure 15). As the total thickness remains unaltered, this observation can be easily explained by change in longitudinal stiffness in a similar way to figure 13. In figure 16, the relative co-efficient of variation (RCOV) (normalized ratio of the standard deviation and mean) for combined stochasticity in micro-mechanical properties are furnished with respect to  $m$ ,  $n$  and  $\theta$  for the first three natural frequencies, wherein clear trends can be observed. It is noticed that the maximum value of RCOV is obtained when the value of  $m$  is 24 while in case of  $n$  the RCOV becomes minimum when  $n$  is 26. For ply orientation angle ( $\theta$ ), the minimum RCOV is observed for  $\theta = 45^\circ$ . It is interesting to notice that the RCOV value increases for both increasing and decreasing  $\theta$  with respect to  $\theta = 45^\circ$ , following similar pattern and reaches the maximum at  $\theta = 0^\circ$  and  $\theta = 90^\circ$ . As RCOV of a system increases, the response bound also increases and subsequently the uncertainty associated with the system



**Fig. 14** (a-c) Probability density function plots for first three natural frequencies corresponding to various numbers of ply numbers having ply orientation angle of  $90^\circ$  ( $n$ )

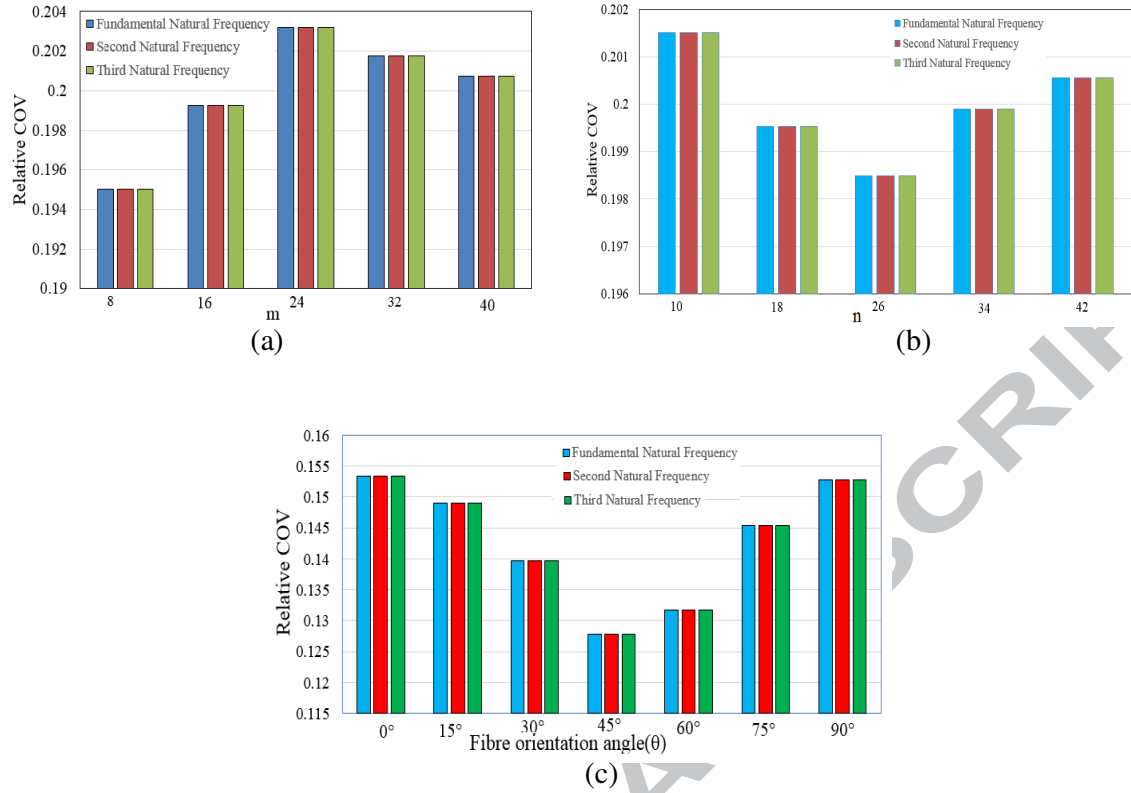
responses increases as well. Thus the analyses presented in the form of RCOV for different laminate configurations has an important role in robust design and control of the structure. Figure 17 (a-c) shows the probability density function plots for first three natural frequencies with respect to different degree of irregularity. The response bounds are found to be increasing with increasing degree of stochasticity with marginal change in the mean values, while the response bounds are observed to be higher for stochasticity in micro-mechanical properties compared to macro-mechanical properties, similar to figure 12. Figure 17(d) shows the probability density function for effective longitudinal modulus ( $E_{eff}$ ), based on which the natural frequencies are obtained. Similar trends as the natural frequencies are noticed in the probabilistic characteristics of  $E_{eff}$ , as expected. Figure 18 (a-c) show the effect of crack density on natural frequencies due to combined variation in micro-mechanical properties. In this article,



**Fig. 15** (a-c) Probability density function plots for first three natural frequencies corresponding to various numbers of ply numbers having ply orientation angle of  $\theta(m)$

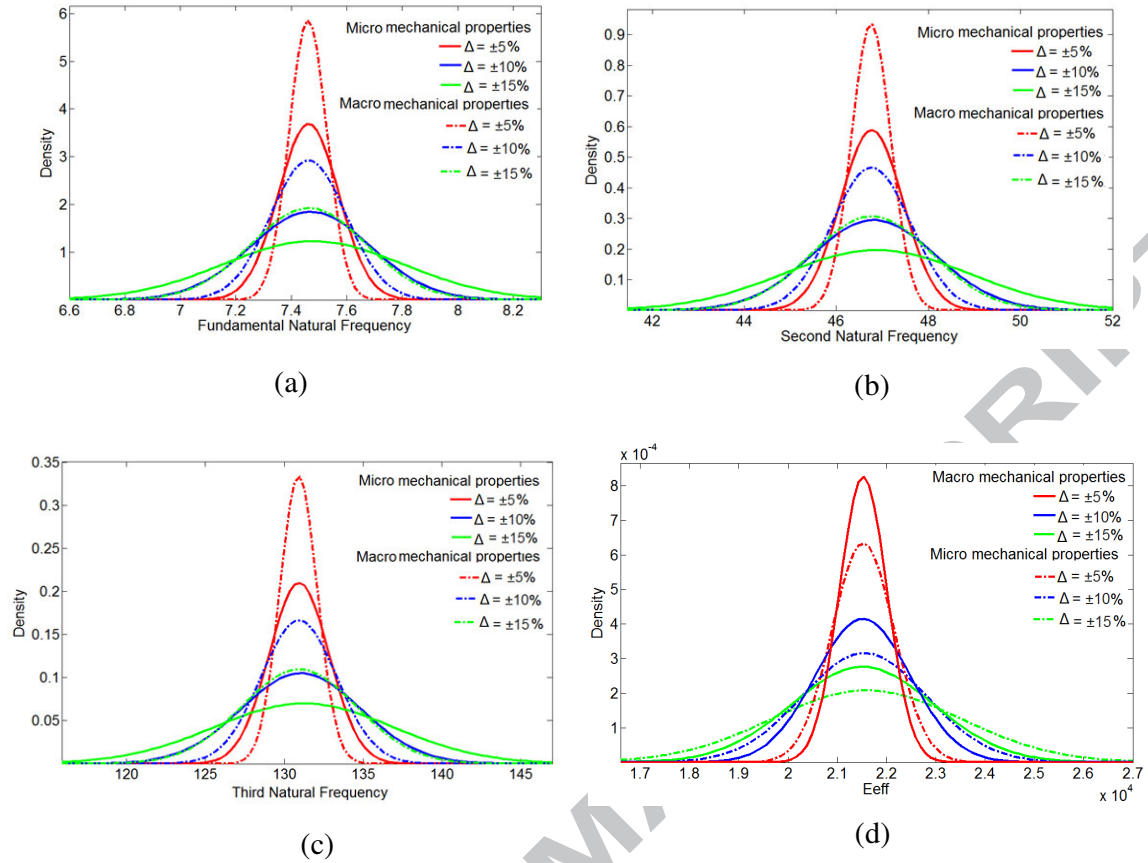
crack density has been defined as number of cracks ( $N$ ) in 100 mm length. As the crack density increases, the mean natural frequencies are found to decrease due to a reduction in effective stiffness. The probability density function of  $E_{eff}$  showed in the figure 18(d) which shows similar trend as the natural frequencies.

Figure 19 and figure 20 present the RCOV for individual variation of different stochastic input parameters corresponding to stochasticity in macro and micro mechanical properties, respectively. These figures provide a clear idea about the relative sensitivity of different stochastic input parameters to the natural frequencies and  $E_{eff}$ . In case of stochasticity in macro-mechanical properties, it is found that mass density, longitudinal elastic modulus, shear modulus  $G_{12}$  and transverse elastic modulus (in decreasing order of sensitivity) are most



**Fig. 16** (a) Relative co-efficient of variation (RCOV) considering  $\theta = 30^\circ, m = 8, 16, 24, 32, 40, n = 18$  and variation  $(\Delta) = \pm 10\%$ ; (b) Relative co-efficient of variation (RCOV) with respect to  $n$  for first three natural frequencies considering fibre orientation angle  $\theta = 30^\circ, m = 16, n = 10, 18, 26, 34, 42$  and variation  $(\Delta) = \pm 10\%$ ; (c) Relative co-efficient of variation (RCOV) with respect to fibre angle ( $\theta$ ) for first three natural frequencies considering fibre angle orientation  $\theta = 0^\circ, 15^\circ, 30^\circ, 45^\circ, 60^\circ, 75^\circ, 90^\circ, m = 16, n = 18$  and variation  $(\Delta) = \pm 10\%$ .

sensitive to the first three natural frequencies and  $E_{eff}$ . For stochasticity in micro-mechanical properties, it is observed that the most sensitive parameters according to decreasing order of sensitivity are longitudinal elastic modulus of fiber, mass density of fiber, volume fraction, mass density of matrix, shear modulus of matrix and elastic modulus of matrix respectively. The results are in good agreement for the natural frequencies and effective longitudinal modulus ( $E_{eff}$ ). Outcomes of the sensitivity analyses can serve as a valuable guideline for efficient uncertainty quantification and subsequent design and control of such structures.



**Fig. 17** (a-c) Probability density function plots for first three natural frequencies considering different degree of stochasticity ( $\Delta$ ); (d) Probability density function plot for the effective longitudinal modulus considering different degree of stochasticity ( $\Delta$ )

Figures 21-23 present the probabilistic description of first three natural frequencies for spatially random variation of only micro-material properties, only crack densities and combined variation of micro-material properties and crack densities, respectively (randomly inhomogeneous system). Results have been presented for different values of stochastic characteristic lengths ( $r$ ) considering mean crack density of 35 with degree of stochasticity  $\Delta = \pm 10\%$ ,  $\theta = 30^\circ$ ,  $m = 16$  and  $n = 18$ . It is interesting to notice that as the value of  $r$  decreases, standard deviation and response bound of the natural frequencies also decrease. In this context, it is to be noted that for the stochasticity category of randomly homogeneous system,  $r = 1$ . The figures also reveal that variation of micro-mechanical properties lead to more deviation in the response bounds compared to crack densities. However, the combined

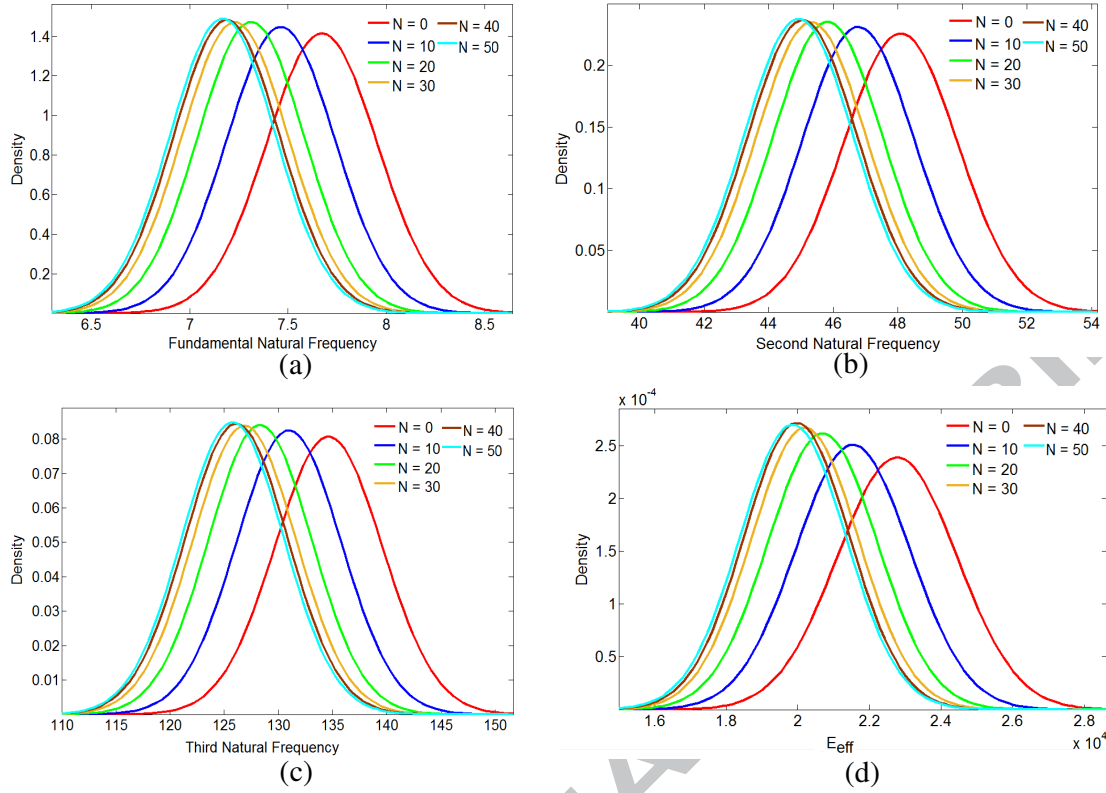


**Fig. 18** (a-c) Probability density function plot for first three natural frequencies, considering different crack densities ( $N$ ), with fibre orientation angle  $\theta = 30^\circ$ ,  $m = 16$ ,  $n = 18$ , degree of stochasticity ( $\Delta$ ) =  $\pm 10\%$  in micro-mechanical properties (d) Probability density function plot for effective longitudinal modulus ( $E_{eff}$ ) considering different crack densities, with fibre orientation angle  $\theta = 30^\circ$ ,  $m = 16$ ,  $n = 18$  and degree of stochasticity ( $\Delta$ ) =  $\pm 10\%$  in micro-mechanical properties

effect of spatially random variation of both micro-mechanical properties and crack densities leads to maximum deviation in the response bound of natural frequencies.

A spatial sensitivity analysis for crack density has been carried out to ascertain the effect of matrix cracking to the first three natural frequencies following variance based sensitivity analysis [54]. The result presented in figure 24 reveals an interesting trend of the sensitivity along length of the beam that the spatial sensitivity of a particular mode of frequency varies following its respective mode shape. Such analysis provides a clear understanding regarding the requirement of adopting necessary measures to identify damages in a particular zone along the length of the beam, according to the vibration mode of interest.

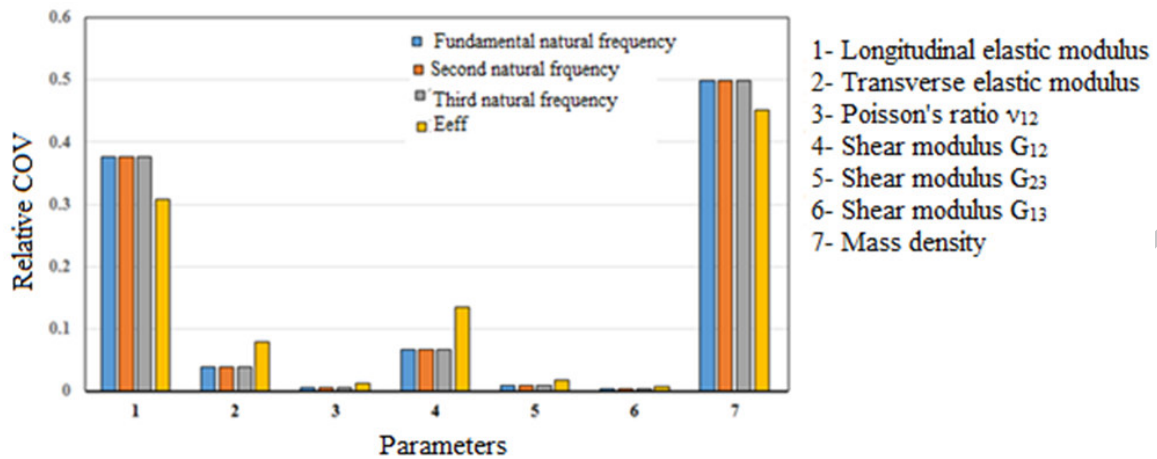


**Fig. 19** Relative co-efficient of variation (RCOV) for the first three natural frequencies and  $E_{eff}$  considering macro-mechanical properties

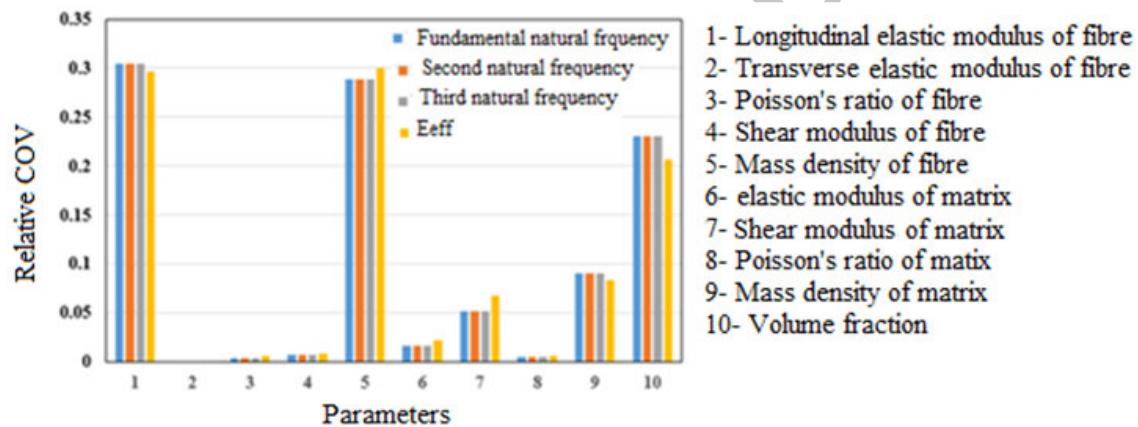
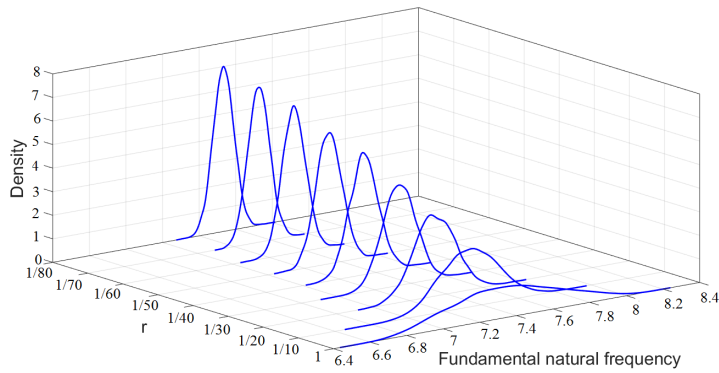
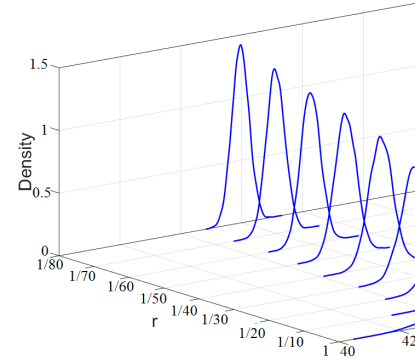


**Fig. 20** Relative co-efficient of variation (RCOV) for the first three natural frequencies and  $E_{eff}$  considering micro-mechanical properties

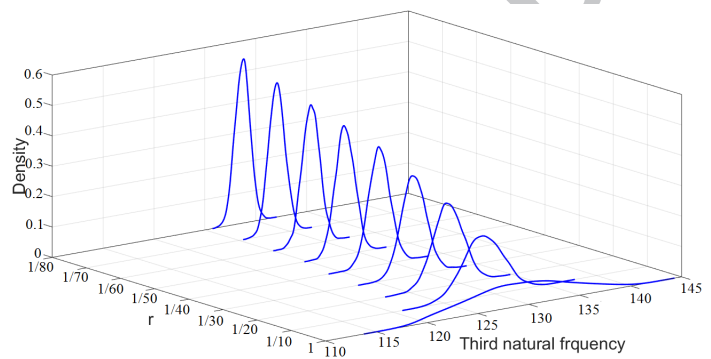
The probability distributions for higher modes of natural frequencies (first eight) corresponding to the bending modes presented in figure 25. In the inset, normalized natural frequencies with respect to their respective mean values are shown. Even though the response bounds of the normalized values do not vary significantly from each other, there is a clear increasing trend of response bounds and standard deviations with respect to actual values for higher modes of vibration. It is evident from the figure that the line connecting the vertices of the probability density function plots for different modes of frequencies follow an exponential



(a)

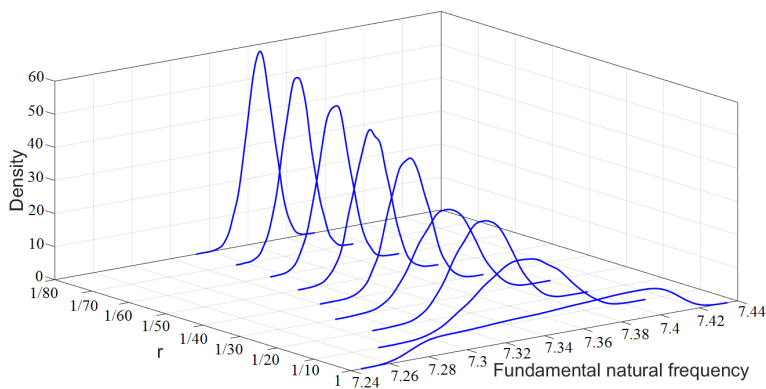


(b)

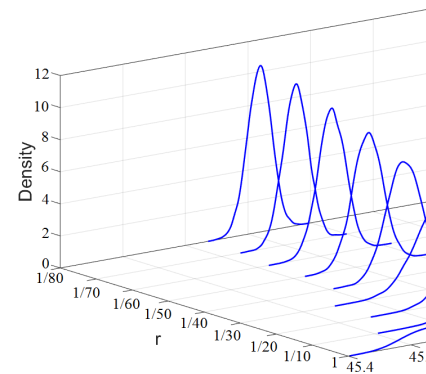


(c)

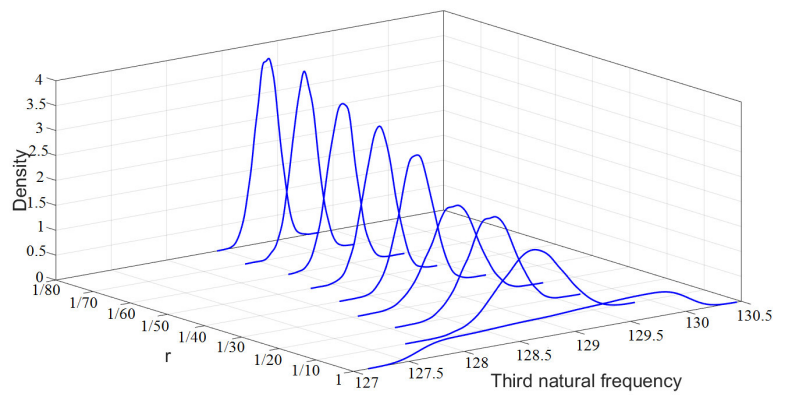
**Fig. 21** Probability density function plots for first three natural frequencies considering spatially random variation



(a)

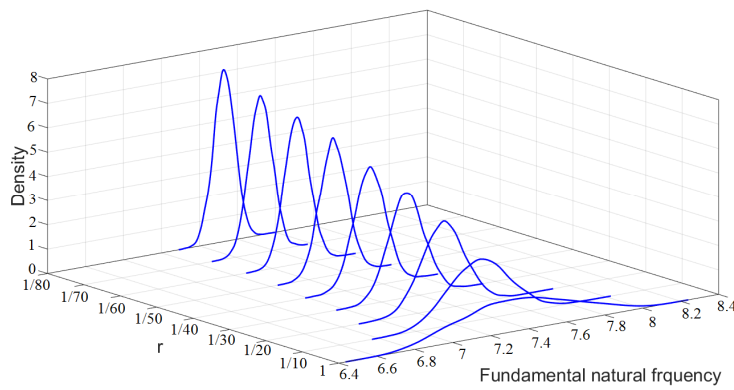


(b)

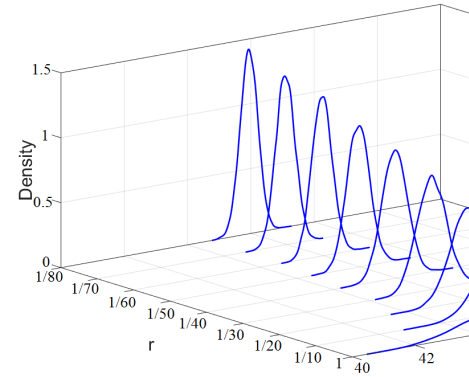


(c)

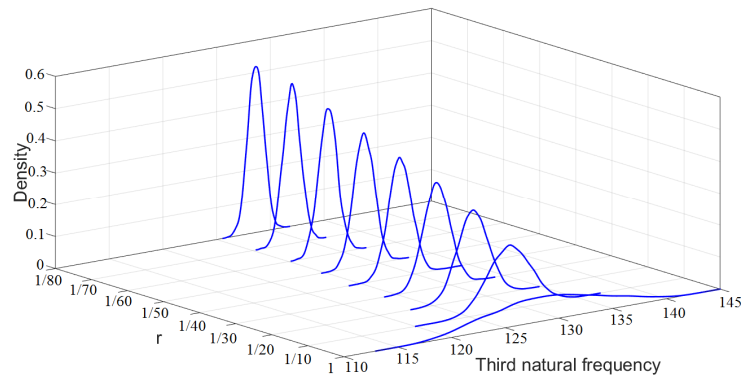
**Fig. 22** Probability density function plots for first three natural frequencies considering spatially random var



(a)



(b)



(c)

**Fig. 23** Probability density function plots for first three natural frequencies considering combined spatially random properties and crack densities

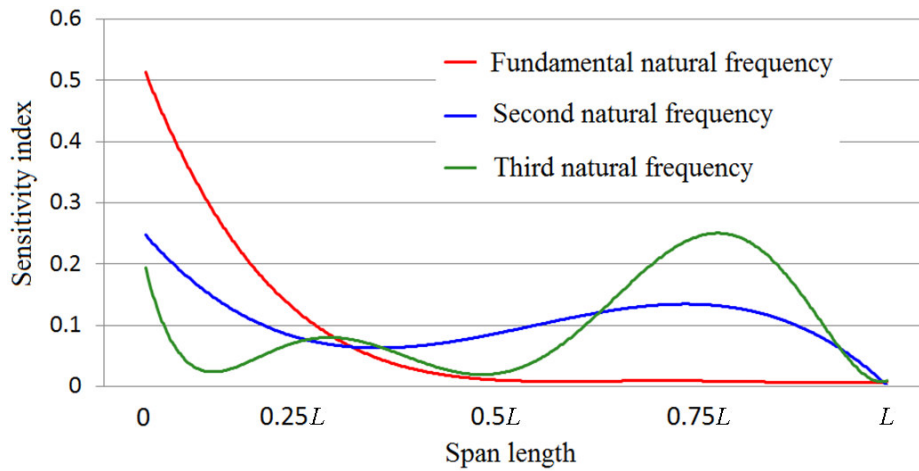


**Fig. 24** Spatial sensitivity of crack density to first three natural frequencies

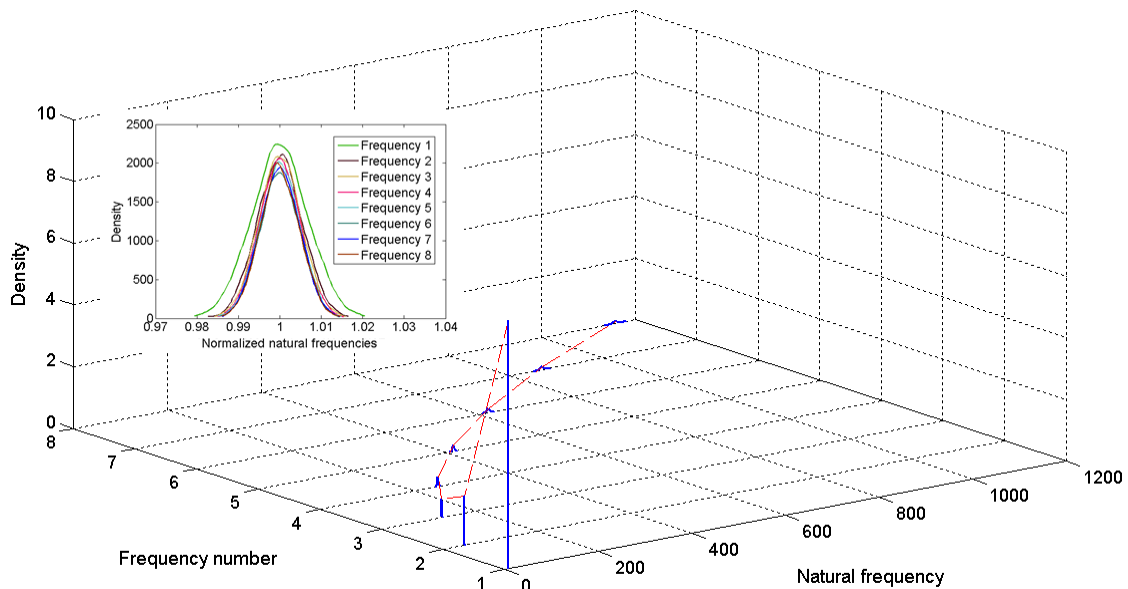


**Fig. 25** Probability density function plots for the first eight natural frequencies corresponding to bending modes. In the inset, normalized natural frequencies with respect to their respective mean values are shown.

decay. Such behaviour for a regular shaped structure is quite in good agreement with the random matrix theory [55].

Figure 26-27 show the effect of noise on RBF based uncertainty quantification algorithm for the thin-walled laminated composite beam. The scatter plots in figure 26 show that the prediction capability of RBF gets increasingly affected by increasing level of noise

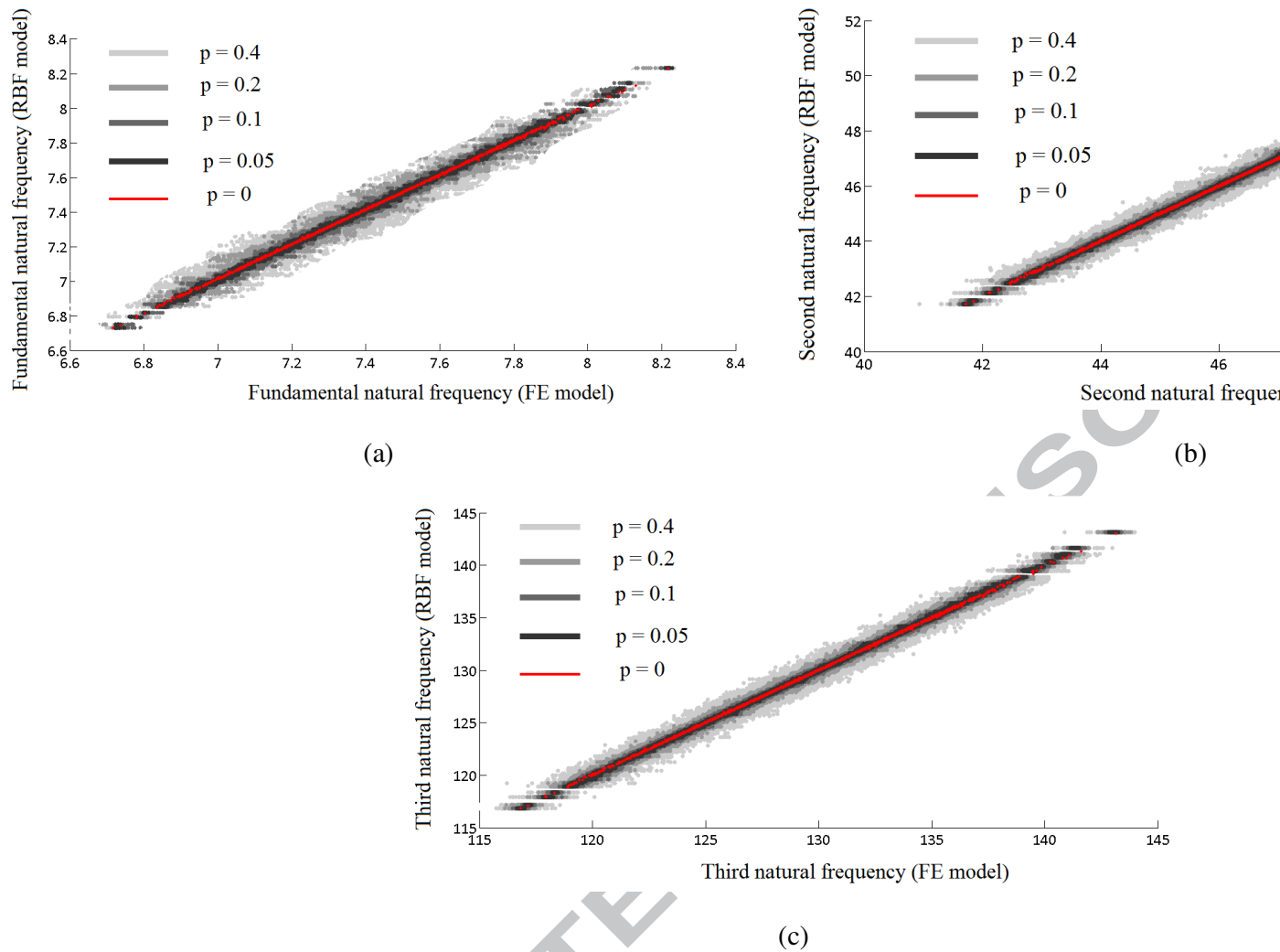
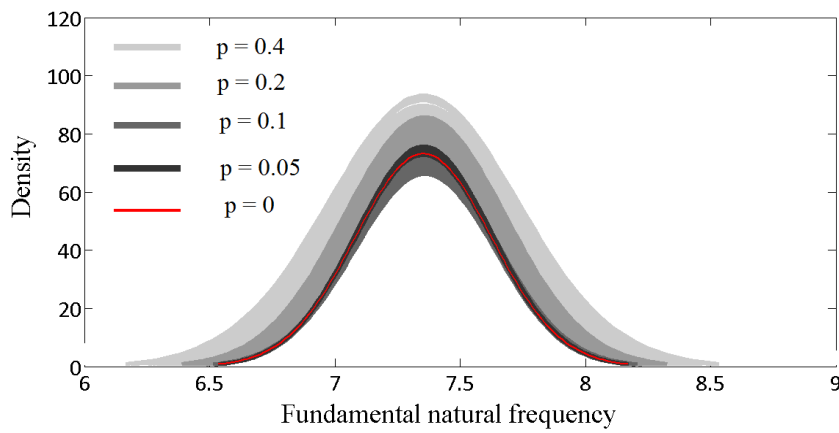
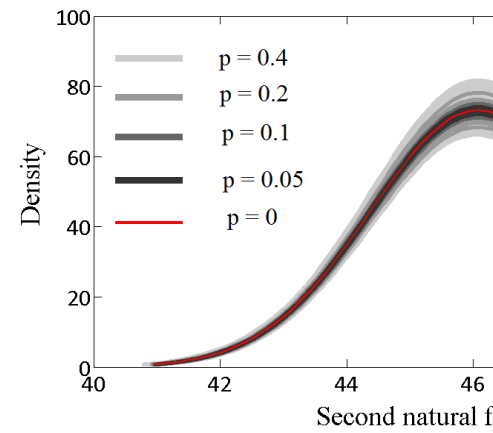


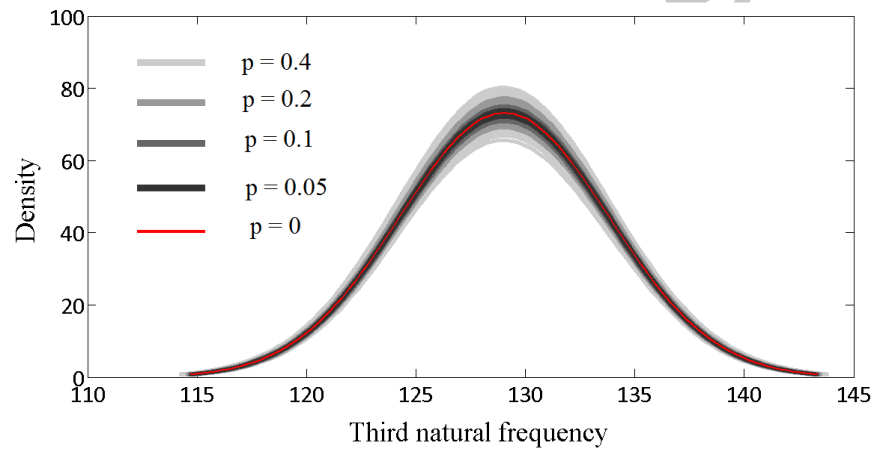
**Fig. 26** Scatter plots depicting the effect of noise on RBF based uncertainty quantification for first three natural frequencies.



(a)



(b)



(c)

**Fig. 27** Probability density function plots depicting the effect of noise on RBF based uncertainty quantification for

( $p$ ), while figure 27 presents the effect of noise on probabilistic description of first three natural frequencies. The fundamental natural frequency is identified to be the most noise sensitive among the first three modes of vibration.

## 6. Summary and perspective

This article presents a stochastic multi-scale bottom-up approach for analyzing damaged thin-walled composite beams (randomly inhomogeneous systems). A novel concept of SRVE is proposed in this context to analyze spatially varying structural systems in conjunction with finite element analysis (the conventional methods of RVE based analyses and analytical solutions for circular beams can not account for the effect of spatially random material and geometric properties). A surrogate based approach (radial basis function) is adopted to achieve computational efficiency in the multi-step analysis. Two separate analyses have been carried out considering stochasticity in micro-mechanical properties and macro-mechanical properties to present comparative results by highlighting the cascading effect of stochasticity. The results are furnished for two different classes of stochasticity: randomly homogeneous system and randomly inhomogeneous system, followed by insightful comparative discussions.

In the micro-mechanical analysis, stochasticity is considered in the micro-mechanical material properties of composites. Effect of spatially random matrix cracking damage (typically a meso-scale attribute) is incorporated in a stochastic framework. Based on the proposed SRVE based approach the equivalent material properties at macro-scale are calculated by accounting the stochasticity in micro-mechanical properties and spatially random matrix cracking damage. Thereby, the equivalent material properties (macro-scale) are fed into the finite element code to obtain the natural frequencies of the structure. In the proposed analysis, stochasticity is accounted at the micro-level first, and then the effect is propagated to the macro-level to characterize the global responses of the structure as shown in figure 12.

Therefore, the present analysis deals with properties and responses at different length scales (micro, meso and macro). It is common in the scientific literature [56] to refer such analysis of composites considering representative volume element as multi-scale analysis. As stochastic system parameters have been accounted in the present study, the analysis is referred as stochastic multi-scale analysis in this paper.

Results are presented from a generalized viewpoint considering spatially random matrix cracking damage to characterize the probabilistic descriptions of natural frequencies. Thus the results in this paper capture the effect of both manufacturing uncertainty (random material properties) and the uncertainty caused during the service life of the structure (spatially varying matrix cracking). While in-depth analyses are presented for the first three natural frequencies, the probabilistic descriptions of higher frequencies are also furnished considering their relevancy of different aerospace and mechanical structures. The standard deviations of the natural frequencies due to stochasticity in micro-mechanical properties are found to be higher than that due to stochasticity in macro-mechanical properties, while the mean remains unaltered. A general tendency of increasing standard deviation and response bound for the first three natural frequencies is noticed with higher degree of stochasticity in the input parameters. The mean of natural frequencies is observed to decrease with the increase in crack density. Sensitivity analyses have been presented from two different perspectives. Sensitivity analysis of different material properties reveal that longitudinal elastic modulus and mass density are the most sensitive parameters for first three natural frequencies in macro-mechanical analysis, while longitudinal elastic modulus of fibre, mass density of fibre and volume fraction are the most important factors for micro-mechanical analysis. The second form of sensitivity analysis considering spatially varying matrix cracking damage reveals an interesting observation that the sensitivity of matrix cracking damage to the natural frequencies along the length of the beam follows the respective mode shapes for first three natural frequencies. From the

developed algorithm for analyzing the effect of noise in RBF based uncertainty quantification, the fundamental natural frequency is found to be the most noise sensitive compared to others. The sensitivity analyses results will allow the designers, manufacturers and maintenance personnel to ensure effective quality control of the structure.

## 7. Conclusions

A bottom-up stochastic analysis is presented for quantifying uncertainty in natural frequencies of damaged thin-walled laminated composite circular beams considering stochasticity in micro-mechanical material properties. The effect of spatially varying matrix cracking damage is analysed along with stochastic material properties following a multi-scale framework. A novel concept of stochastic representative volume element (SRVE) is proposed to consider the spatially varying structural attributes effectively. In this study, the probability distributions of first three natural frequencies due to stochasticity in micro-mechanical properties have been compared with that due to same degree of stochasticity in macro-mechanical properties to ascertain the cascading effect of uncertainty propagation. Sensitivity of different micro and macro mechanical properties has been analyzed for the first three natural frequencies. Another form of sensitivity analysis is presented showing the spatial sensitivity of matrix crack location along the length of the beam for the first three natural frequencies. To achieve computational efficiency, a radial basis function based uncertainty quantification algorithm has been developed in this study, wherein it is observed that the required number of original finite element simulations can be significantly reduced. Effect of noise on the proposed uncertainty quantification algorithm has been presented considering different levels of noise, wherein it is noticed that the fundamental natural frequency is most affected by such simulated noise.

The results presented in this paper provide a thorough insight on the effects of stochasticity in micro and macro mechanical properties of damaged laminated composite

beams considering two different classes of stochasticity: randomly homogeneous system and randomly inhomogeneous system. Thus both the forms of uncertainties caused during manufacturing (stochastic material properties) and service life (matrix cracking) of the structure have been quantified. Such stochasticity/ system irregularities have considerable effect on the dynamic responses of the structure. Thus it is imperative to take into account the effect of these uncertainties in subsequent analyses and design for ensuring robust and sustainable system performance. Novelty of this article includes the consideration of spatially random variation of material properties and crack density following the SRVE based approach. The concept of SRVE is quite general in nature, thus it can be extended to other structures and stochastic systems with spatial variability in two and three dimensions. Moreover, the proposed computationally efficient RBF based framework for uncertainty quantification in thin-walled composite beams can be extended to other structures for characterizing various global stochastic responses in future.

### Acknowledgements

SN and SS are grateful for the support provided through the Lloyd's Register Foundation Centre. The Foundation helps to protect life and property by supporting engineering-related education, public engagement and the application of research.

### References

1. Sriramula S, Chryssanthopoulos K M, Quantification of uncertainty modelling in stochastic analysis of FRP composites, *Composites Part A: Applied Science and Manufacturing*, 40 1673-1684, 2009
2. Oberkampf W L, Helton J C, Sentz K, Mathematical representation of uncertainty, *In: 42nd AIAA/ASME/ASCE/AHS/ASC structures, structural dynamics, and materials conference and exhibit*, Seattle, WA; 2001
3. Agarwal H, Renaud J E, Preston E L, Padmanabhan D, Uncertainty quantification using evidence theory in multidisciplinary design optimization, *Reliability Engineering & System Safety*, 85 281-94, 2004
4. Shaw A, Sriramula S, Gosling P D, Chryssanthopoulos M K, A critical reliability evaluation of fibre reinforced composite materials based on probabilistic micro and macro-mechanical analysis, *Composites Part B: Engineering*, 41 6 446-453, 2010

5. Bank L C, Bednarczyk P J, A Beam Theory for Thin-walled Composite Beams, *Composites Science and Technology*, 32 265-277, 1988
6. Chandra R, Stemple A D, Chopra I, Thin-walled composite beams under bending, torsional, and extensional loads, *Journal of Aircraft*, 27 (7) 619-626, 1990
7. Bauld N, Tzeng L. A Vlasov, Theory for fiber-reinforced beams with thin-walled open cross sections, *International Journal of Solids and Structures*, 20(3) 277–297, 1984
8. Bauchau O, A beam theory for anisotropic materials, *Journal of Applied Mechanics*, 52(2) 416–22, 1985.
9. Cortínez VH, Piován M, Vibration and buckling of composite thin-walled beams with shear deformability, *Journal of Sound and Vibration*, 258(4) 701–23, 2002
10. Librescu L, Song O, On the aeroelastic tailoring of composite aircraft swept wings modeled as thin-walled beam structures. *Composites Eng*, 2(5–7) 497–512, 1992
11. Song O, Librescu L. Free vibration of anisotropic composite thin-walled beams of closed cross-section contour, *Journal of Sound and Vibration*, 167(1) 129–47, 1993.
12. Rehfield L, Atilgan A, Hodges D, Non-classical behavior of thin-walled composite beams with closed cross sections, *Journal of the American Helicopter Society*, 35(3) 42–50, 1990
13. Chakrabarti A, Sheikh A. H., Griffith M., Oehlers D. J., Dynamic Response of composite beams with partial shear interactions using a higher order beam theory. *Journal of Structural Engineering*, 139 (1), 47-56, 2013
14. Chakrabarti A, Chalak H D, Iqbal M A and Sheikh A H, A new FE model based on higher order zigzag theory for the analysis of laminated sandwich beam with soft core. *Composite Structures*, 93(2), 271-279, 2011
15. Giunta G, Biscani F, Belouettar S, Ferreira AJM, Carrera E, Free vibration analysis of composite beams via refined theories, *Composites Part B: Engineering*, 44(1) 540–52, 2013
16. Carrera E, Giunta G, Petrolo M, *Beam structures: classical and advanced theories*, Wiley, 2011.
17. Dey S., Mukhopadhyay T., Spickenheuer A., Adhikari S., Heinrich G., Bottom up surrogate based approach for stochastic frequency response analysis of laminated composite plates, *Composite Structures*, 140 712–727, 2016
18. Dey S., Mukhopadhyay T., Khodaparast H. H., Adhikari S., Stochastic natural frequency of composite conical shells, *Acta Mechanica*, 226 (8) 2537-2553, 2015
19. Dey S., Naskar S., Mukhopadhyay T., Gohs U., Spickenheuer A., Bittrich L., Sriramula S., Adhikari S., Heinrich G., Uncertain natural frequency analysis of composite plates including effect of noise – A polynomial neural network approach, *Composite Structures*, 143 130–142, 2016
20. Piován M T, Ramirez J M, Sampaio R, Dynamics of thin-walled composite beams: Analysis of parametric uncertainties, *Composite Structures*, 105 14–28, 2013
21. Singh C V, Multiscale modeling of damage in multidirectional composite laminates, PhD Thesis, Texas A&M University, 2008
22. Hardy R L, Theory and applications of the multiquadric-biharmonic method, *Comput. Math. Appl*, 29 163{208}, 1990
23. Powell M J D, Radial basis functions for multivariable interpolation: a review, *Algorithms for Approximation*, Mason J.C., Cox M.G. (eds.), London, Oxford University Press, 1987
24. Nuismer, R. J., Tan, S. C., Constitutive relations of a cracked composite lamina, *J Compos Mater*, 22, 306–321, 1988
25. Jones R M, *Mechanics of Composite structures*, Taylor & Francis, Philadelphia, PA, 1999

26. Polyzois D., Raftoyiannis G., Ibrahim S., Finite Elements for the Dynamic Analysis of Tapered Composite Poles, *Composite Structures*, 43 25–34, 1998
27. Ferrero J F, Barrau J J, Segura J M, Sudre M, Castanie B, Analytical theory for an approach calculation of non-balanced composite box beams, *Thin-Walled Struct.*, 39 709–729, 2001
28. Estivalezes E, Barrau J J, Analytical theory for an approach calculation of composite box beams subjected to tension and bending, *Composites. Part B*, 29 371–376, 1998
29. Chandrupatla T R, Belegundu A D, Introduction to Finite Elements in Engineering, *Prentice-Hall*, Englewood Cliffs, 2001
30. Kansa E J, Hon Y C, Circumventing the Ill-Conditioning Problem with Multiquadric Radial Basis Functions, *Comput. Math. Appl.*, 39 123–137, 2000
31. Queipo N V, Haftka R T, Shyy W, Goel T, Vaidyanathan R, Tucker P K, Surrogate-based analysis and optimization, *Progress in Aerospace Sciences*, 41 1-28, 2005
32. Powell M J D, Radial basis functions for multivariable interpolation: a review, *Algorithms for Approximation*, Mason J.C., Cox M.G. (eds.), London, Oxford University Press, 1987
33. Krishnamurthy, T., Response surface approximation with augmented and compactly supported radial basis functions, *The 44th AIAA/ASME/ASCE/AHS/ASC structures, structural dynamics, and materials conference*, Norfolk, VA, 2003
34. Carrere N, Rollet, Y., Leroy, F. H., Maire, J. F., (2009), Efficient structural computations with parameters uncertainty for composite applications, *Compos Sci Technol*, 69, 1328–1333
35. Liu G R, Wang J G, A Point Interpolation Meshless Method Based on Radial Basis Functions, *Int. J. Num. Meth. Eng.*, 54 1623–1648, 2002
36. Ferreira A J M, Fasshauer G E, Analysis of natural frequencies of composite plates by an RBF-pseudo spectral method, *Composite structures*, 79 202–210, 2007
37. Powell M J D, Radial basis functions for multivariable interpolation: a review, *Algorithms for Approximation*, Mason J.C., Cox M.G. (eds.), London, Oxford University Press, 1987
38. Krishnamurthy, T., Response surface approximation with augmented and compactly supported radial basis functions, *The 44th AIAA/ASME/ASCE/AHS/ASC structures, structural dynamics, and materials conference*, Norfolk, VA, 2003
39. Beatson R K, Fast Fitting of Radial Basis Functions: Methods Based on Preconditioned gmres Iteration, *Advances in Computational Mathematics*, 11 253–270, 1999
40. Fasshauer G E, Solving Partial Differential Equations by Collocation with Radial Basis Functions, Surface Fitting and Multiresolution Methods, Vol. 2, *Proceedings of the 3rd International Conference on Curves and Surfaces*, 2 131–138, 1997
41. Hon Y C, Mao X Z, On Unsymmetric Collocation by Radial Basis Functions, *Applied. Math. Computation.*, 119 177–186, 2001
42. Kansa E J, Multiquadrics: A Scattered Data Approximation Scheme with Applications to Computational Fluid Dynamics. I: Surface Approximations and Partial Derivative Estimates, *Comput. Math. Appl.*, 19 127–145, 1990
43. Kansa E J, Multiquadrics: A Scattered Data Approximation Scheme with Applications to Computational Fluid Dynamics. II: Solutions to Parabolic, Hyperbolic and Elliptic Partial Differential Equations, *Comput. Math. Appl.*, 19 147–161, 1990
44. Mukhopadhyay T., Adhikari S., Equivalent in-plane elastic properties of irregular honeycombs: An analytical approach, *International Journal of Solids and Structures*, 91 169–184, 2016
45. Mukhopadhyay T., Adhikari S., Effective in-plane elastic properties of auxetic honeycombs with spatial irregularity, *Mechanics of Materials*, 95 204–222, 2016

46. McKay MD, Beckman RJ, Conover WJ. A comparison of three methods for selecting values of input variables in the analysis of output from a computer code. *Technometrics*, 42(1) 55–61, 2000
47. Sobol' IM. On the distribution of points in a cube and the approximate evaluation of integrals, *USSR Comput Math Math Phys*, 7 86–112, 1967
48. Mukhopadhyay T., Chowdhury R., Chakrabarti A., Structural damage identification: A random sampling-high dimensional model representation approach, *Advances in Structural Engineering*, 19(6) 908–927, 2016
49. Mukhopadhyay T., Naskar S., Dey S., Adhikari S., On quantifying the effect of noise in surrogate based stochastic free vibration analysis of laminated composite shallow shells, *Composite Structures*, 140 798–805, 2016
50. Mukhopadhyay T., A multivariate adaptive regression splines based damage identification methodology for web core composite bridges including the effect of noise, *Journal of Sandwich Structures & Materials* (In Press)
51. Mukhopadhyay T., Chakraborty S., Dey S., Adhikari S., Chowdhury R., A critical assessment of Kriging model variants for high-fidelity uncertainty quantification in dynamics of composite shells, *Archives of Computational Methods in Engineering*, DOI: 10.1007/s11831-016-9178-z
52. Soden P D, Hinton M J, Kaddour A S, Lamina properties, lay-up configurations and loading conditions for a range of fibre reinforced composite laminates, *Compos. Sci. Technol.*, 58 (7) 1011-1022, 1998 //51
53. Giraitis L, Surgailis D, A central limit theorem for quadratic form in strongly dependent linear variables and its application to Whittle's estimate, *Probability Theory and Related Fields*, 86 87-140, 1990
54. Dey S., Mukhopadhyay T., Adhikari S., Stochastic free vibration analysis of angle-ply composite plates - A RS-HDMR approach, *Composite Structures*, 122 526–536, 2015
55. Pastur L., Shcherbina M., Eigenvalue Distribution of Large Random Matrices, *Mathematical Surveys and Monographs*, Volume 171, 2011
56. May M, Nossek M, Petrinic N, Hiermaier S, Thoma K, Adaptive multi-scale modeling of high velocity impact on composite panels, *Composites: Part A*, 58, 56–64, 2014